



Natural Resources  
Canada

Ressources naturelles  
Canada

**GEOLOGICAL SURVEY OF CANADA  
OPEN FILE 8565**

**Detrital U-Pb zircon and  $^{40}\text{Ar}/^{39}\text{Ar}$  muscovite geochronology  
of the Whitehorse Trough, and surrounding rocks, Yukon  
and British Columbia**

**D. A. Kellett and P. Iraheta Muniz**

**2019**

**Canada**



## **GEOLOGICAL SURVEY OF CANADA OPEN FILE 8565**

# **Detrital U-Pb zircon and $^{40}\text{Ar}/^{39}\text{Ar}$ muscovite geochronology of the Whitehorse Trough, and surrounding rocks, Yukon and British Columbia**

**D. A. Kellett<sup>1</sup> and P. Iraheta Muniz<sup>2</sup>**

<sup>1</sup>Geological Survey of Canada, 1 Challenger Drive, Dartmouth, Nova Scotia B2Y 4A2

<sup>2</sup>Geological Survey of Canada, 601 Booth Street, Ottawa, Ontario K1A 0E8

**2019**

© Her Majesty the Queen in Right of Canada, as represented by the Minister of Natural Resources, 2019

Information contained in this publication or product may be reproduced, in part or in whole, and by any means, for personal or public non-commercial purposes, without charge or further permission, unless otherwise specified.

You are asked to:

- exercise due diligence in ensuring the accuracy of the materials reproduced;
- indicate the complete title of the materials reproduced, and the name of the author organization; and
- indicate that the reproduction is a copy of an official work that is published by Natural Resources Canada (NRCan) and that the reproduction has not been produced in affiliation with, or with the endorsement of, NRCan.

Commercial reproduction and distribution is prohibited except with written permission from NRCan. For more information, contact NRCan at [rncan.copyrightdroitdauteur.rncan@canada.ca](mailto:rncan.copyrightdroitdauteur.rncan@canada.ca).

Permanent link: <https://doi.org/10.4095/314694>

This publication is available for free download through GEOSCAN (<https://geoscan.nrcan.gc.ca/>).

### **Recommended citation**

Kellett, D.A., and Iraheta Muniz, P., 2019. Detrital U-Pb zircon and  $^{40}\text{Ar}/^{39}\text{Ar}$  muscovite geochronology of the Whitehorse Trough, and surrounding rocks, Yukon and British Columbia; Geological Survey of Canada, Open File 8565, 35 p. <https://doi.org/10.4095/314694>

## CONTENTS

<b>INTRODUCTION</b> .....	2
<b>REGIONAL GEOLOGICAL FRAMEWORK</b> .....	2
<b>U-Pb ANALYTICAL METHODS</b> .....	4
<b><sup>40</sup>Ar/<sup>39</sup>Ar ANALYTICAL METHODS</b> .....	4
<b>ACKNOWLEDGMENTS</b> .....	5
<b>U-Pb RESULTS</b> .....	6
<b><sup>40</sup>Ar/<sup>39</sup>Ar RESULTS</b> .....	29
<b>REFERENCES</b> .....	31

## INTRODUCTION

This multicomponent Open File presents detrital zircon U-Pb (11 samples) and detrital muscovite  $^{40}\text{Ar}/^{39}\text{Ar}$  (2 samples) results for sedimentary rocks sampled from select units of the Lewes River Group/Stuhini Group, Laberge Group, Bowser Lake Group and Tantalus Formation in southern Yukon and northern British Columbia, as well as one quartzofeldspathic schist sample from the Florence Range metamorphic rocks associated with the Yukon Tanana terrane. Sample locations are shown in Figure 1. This analytical work was conducted as part of the Yukon Tectonic Evolution activity of the GEM (Geomapping for Energy and Minerals) program of the Geological Survey of Canada (see Kellett et al., 2017; Kellett et al., 2018 for details).

Interpretations of the U-Pb and  $^{40}\text{Ar}/^{39}\text{Ar}$  results for individual rock samples are given below in the Results section of this report. Representative transmitted light and back-scattered electron (BSE)/cathodoluminescence (CL) zircon images are shown for each sample, and U-Pb detrital zircon results are illustrated by Concordia and combined histogram/probability density diagrams.  $^{40}\text{Ar}/^{39}\text{Ar}$  detrital muscovite results are presented in kernel density estimate plots (Vermeesch, 2012; 2018). The results and age interpretations for all samples presented are summarized in Table 1 (separate file). The full U-Pb and  $^{40}\text{Ar}/^{39}\text{Ar}$  datasets are provided as separate Microsoft Excel files in Appendices A and B, respectively. Plots of the full step heat  $^{40}\text{Ar}/^{39}\text{Ar}$  spectra for each single crystal step heat experiment are collated into an Adobe PDF file (Appendix C). Adobe PDF files for each detrital zircon sample containing BSE and CL images for all mounted zircon grains are also presented in Appendix D. Grains are numbered and correspond to analysis spot names; the locations of SHRIMP (sensitive high resolution ion microprobe) analytical spots are depicted by ellipses.

## REGIONAL GEOLOGICAL FRAMEWORK

The Canadian Cordillera is a long-lived and presently active accretionary orogen that has developed against the present day western margin of Laurentia (Coney et al., 1980). The Yukon Tanana continental arc terrane rifted from Laurentia during the late Paleozoic. It amalgamated with related allochthonous island arcs Stikinia and Quesnellia, and eventually accreted back to the Laurentian margin (Fig. 1; Nelson et al., 2013). That accretion, which also included Cache Creek and Slide Mountain oceanic rocks, is thought to have occurred between Late Triassic and Middle Jurassic, and represents the first major Laurentian accretionary event of the northern Canadian Cordillera (Colpron et al., 2015). The clastic sedimentary record spanning this period is currently preserved in southwestern Yukon and northwestern British Columbia (Fig. 1).

The Mesozoic stratigraphy of the Intermontane region of southern Yukon and northwestern British Columbia comprises distinct Triassic, Early-Middle Jurassic, and Middle Jurassic-Early Cretaceous sequences. Triassic clastic deposition occurred on the flank of Stikinia as Sinwa Formation (British Columbia, B.C.), and the Mandanna member of Aksala formation, both representing the uppermost unit of the volcano-sedimentary Stuhini Group (B.C.)/Lewes River Group (Yukon) (English et al., 2005, Shirmohammad et al., 2011). These units are overlain by the Early to Middle Jurassic Laberge Group, a 3 km package of predominantly sandstone, siltstone and conglomerate (Johansson et al., 1997; Hutchison, 2017) that forms the main unit of the Whitehorse trough, a basin that extends for ~600 km along the strike length of the northern Canadian Cordillera (Fig. 1). The Whitehorse trough has been described as a syn-orogenic piggy-back basin formed on the eastern flank of Stikinia (Colpron et al., 2015). Deposition of the Laberge Group was followed by an unconformity, upon which the Bowser Lake Group was deposited in northern B.C., and the Tantalus Formation was deposited in southern Yukon. Evenchick and Thorkelson (2005) and Long et al. (2015) provide detailed descriptions of these two clastic sequences, respectively.

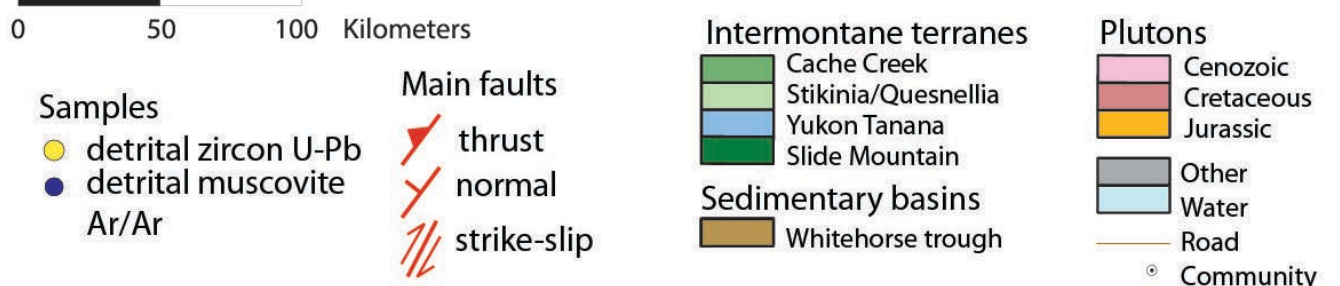
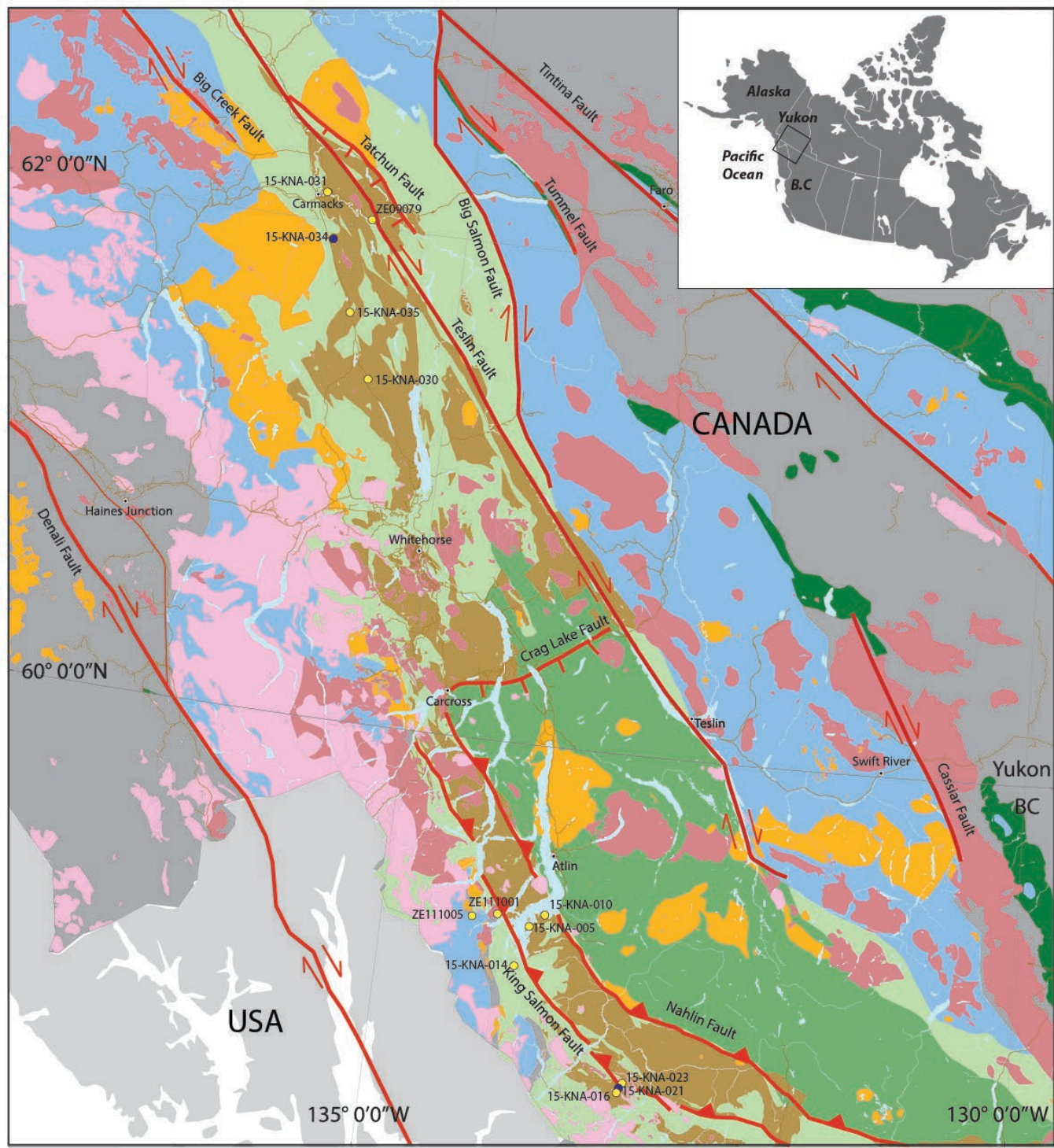


Figure 1: Geological map showing the Intermontane terranes, Whitehorse trough, and Jurassic and younger plutons, southwestern Yukon and northwestern British Columbia. Map shows sample locations for this study. Modified from Cui et al. (2017) and Colpron et al. (2016).

## U-Pb ANALYTICAL METHODS

All samples were disaggregated using standard crushing/pulverizing techniques followed by density separation using a Wilfley table and heavy liquids. A Frantz Magnetic Separator was used to isolate a zircon-rich non-magnetic separate.

SHRIMP analytical procedures followed those described by Stern (1997), with standards and U-Pb calibration methods following Stern and Amelin (2003). Briefly, zircon grains were cast in 2.5 cm diameter epoxy mounts (GSC #582, 641, 798, 922) along with fragments of GSC laboratory standard zircon (z6266, with  $^{206}\text{Pb}/^{238}\text{U}$  age = 559 Ma or z8539/10493 with  $^{206}\text{Pb}/^{238}\text{U}$  age = 417 Ma). The mid-sections of the zircon grains were exposed using 9, 6, and 1  $\mu\text{m}$  diamond compound, and the internal features of the grains (such as zoning, structures, alteration, etc.) were characterized in back-scattered electron mode (BSE) and/or cathodoluminescence mode (CL) utilizing a Zeiss Evo 50 scanning electron microscope (Appendix D). On the mass spectrometer, eleven masses including background were sequentially measured with a single electron multiplier. Off-line data processing was accomplished using SQUID2 (version 2.50.11.10.15, rev. 15 Oct 2011). The  $1\sigma$  external errors of  $^{206}\text{Pb}/^{238}\text{U}$  ratios reported in Appendix A incorporate the error in calibrating the standard. Common Pb correction utilized the Pb composition of the surface blank (Stern, 1997). Details of each analytical session, including spot size, number of scans, primary standard used, and calibration error, are given in the footnotes of Appendix A.

Analyses of secondary zircon reference material were interspersed between sample analyses to verify the accuracy of the U-Pb calibration. The measured  $^{206}\text{Pb}/^{238}\text{U}$  ages of the secondary reference materials are reported for each session in the footnote of Appendix A for comparison against their published, accepted ages. The accepted  $^{206}\text{Pb}/^{238}\text{U}$  age of z8539/10493 is  $416.5\pm 0.22$  Ma, based on 21 isotope dilution thermal ionization mass spectrometry (ID-TIMS) fractions (Black et al., 2004). The accepted  $^{206}\text{Pb}/^{238}\text{U}$  age of z9910 is  $441.2\pm 0.4$  Ma, based on 5 ID-TIMS fractions (B. Davis and V. McNicoll, unpublished data). The accepted  $^{206}\text{Pb}/^{238}\text{U}$  age of z6266 is  $559.0\pm 0.2$  Ma, based on 22 ID-TIMS fractions (Stern and Amelin, 2003).

Isoplot v. 4.15 (Ludwig, 2003) in Microsoft Excel 2016 was used to calculate Concordia ages (including its  $2\sigma$  error, MSWD, and probability of concordance) and weighted mean ages, as well as to generate Concordia and histogram/probability density plots. The error ellipses on the Concordia diagrams and the weighted mean errors are reported at the 95% confidence level. An evaluation of the long term reproducibility of  $^{206}\text{Pb}/^{238}\text{U}$  age of secondary standard 9910 indicates that the minimum reproducibility precision of SHRIMP ion probe weighted mean results is 1% ( $2\sigma$ , based on 51 analytical sessions, B. Davis pers. comm). In cases where the precision of the weighted mean calculation for individual samples falls below this threshold, the weighted mean  $2\sigma$  error is augmented to 1%.

There are many ways to determine the maximum depositional age of a sample based on a population of detrital zircon U-Pb ages (e.g. Dickinson and Gehrels, 2009). For the purposes of this report we focus on the youngest population mode for most samples. In cases where subtle skewness is observed in the youngest ages, Ludwig's (2003) unmix function is used to constrain maximum depositional age. In cases where concordant replicate analyses exist for the youngest grain, a weighted mean of the  $^{206}\text{Pb}/^{238}\text{U}$  age for these replicate analyses is used instead.

## $^{40}\text{Ar}/^{39}\text{Ar}$ ANALYTICAL METHODS

Each sample was crushed using a ceramic mortar and pestle. The highest quality mineral grains were picked from the 250-500  $\mu\text{m}$  fraction and then packed into aluminum foil packets and arranged in 35 mm-long vertical tubes. Several flux monitor grains of Fish Canyon tuff sanidine (FCT-SAN) ( $28.305 \pm 0.036$   $1\sigma$  Ma; Renne et al., 2010) were loaded into each sample packet. J values were interpolated for

samples situated between the spaced FCT-SAN monitor grains. GA 1550 biotite ( $99.77 \pm 0.11$   $1\sigma$  Ma, normalized to FCT-SAN at  $28.305 \pm 0.036$   $1\sigma$  Ma) was used as a secondary standard to confirm the accuracy of the interpolations (Renne et al., 2010). The prepared can was irradiated for 160 MWH in medium flux position 8B at the research nuclear reactor of McMaster University (MNR) in Hamilton, Ontario, Canada. Neutron fluence was  $\sim 0.9 \times 10^{13}$  neutrons/cm<sup>2</sup> operating at a 2.5 MW power level. Correction factors for typical interference species produced by thermal neutrons during irradiation are included in the footnote of Appendix B.

The <sup>40</sup>Ar/<sup>39</sup>Ar analyses were conducted at the Noble Gas Laboratory at the Geological Survey of Canada in Ottawa (Canada). Individual grains were loaded into a copper sample holder placed into a CO<sub>2</sub> laser source chamber under ultrahigh vacuum. A Photon Machines, Inc. Fusions 10.6 55 W CO<sub>2</sub> laser equipped with a beam-homogenizing lens was used to heat each grain for at least 30 seconds per step, and laser power was increased incrementally for each subsequent step. Heating schedules ranged from 0.1 to 7 W and were adjusted with the aim of releasing near equal volumes of <sup>39</sup>Ar among heating steps.

The gas released during each incremental heating step was cleaned for 3–4 minutes using two SAES™ NP-10 getters held at  $\sim 400^\circ\text{C}$ , and a room temperature getter containing HY-STOR® 201 calcium-nickel alloy pellets. The gas was then admitted to a Nu Instruments Limited Noblesse magnetic sector multicollector noble gas mass spectrometer. The Nu Noblesse (model 018) is a single-focusing, Nier-source, 75 magnetic sector multicollector noble gas spectrometer equipped with two quadrupole lens arrays. Ar ions were measured with a fixed array of three ETP® discrete dynode ion-counting multipliers. Data collection followed the measurement scheme MC-Y detailed in Kellett and Joyce (2014). Blanks were run every 5<sup>th</sup> analysis, in an identical manner to unknowns. Air shots were analyzed every 10<sup>th</sup> analysis to monitor efficiency and mass fractionation. Full results including background measurements are included in Appendix B. Sensitivity of the Nu Noblesse at the time of analyses was 7.1-7.5 Amps/mol. Data collection, reduction, error propagation, age calculation and plotting were performed using the software MassSpec (version 7.93) (Deino, 2001). Thorough descriptions of laboratory procedures, instrument specifications, data collection, and correction factors are provided in Kellett and Joyce (2014).

Ages presented here were calculated using an assumed <sup>40</sup>Ar/<sup>36</sup>Ar ratio of 298.56 for atmospheric Ar (Lee et al., 2006) and decay constants and isotopic abundance after Min et al. (2000). Plateau ages met the following criteria: at least three consecutive heating steps that are of equivalent age at the  $2\sigma$  level, and together comprising at least 50% of <sup>39</sup>Ar released. Pseudo-plateau ages were determined by calculating an integrated age for the flattest portion of the step heat spectrum. Integrated ages are an integration of all heating steps. All ages are reported with  $2\sigma$  error.

## ACKNOWLEDGMENTS

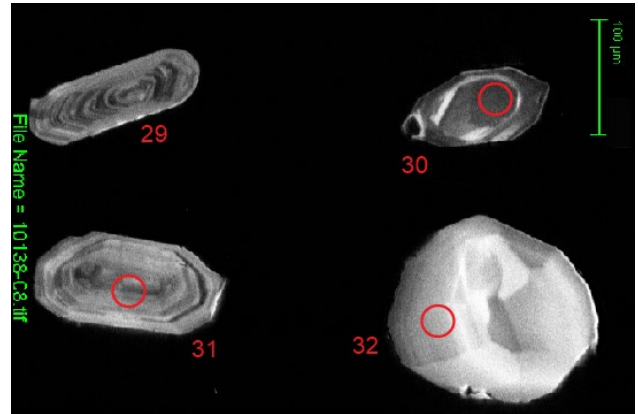
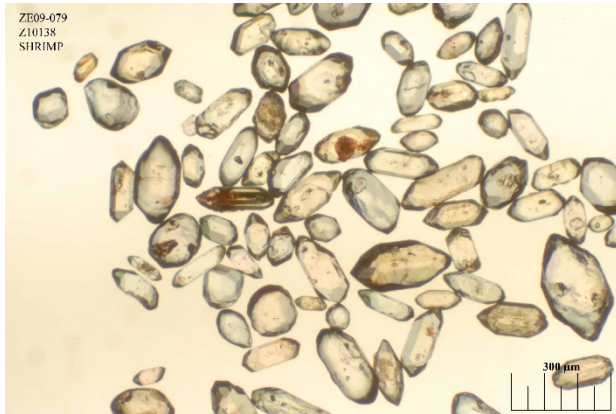
The authors wish to thank N. Rayner, T. Pestaj, N. Joyce, and L. Cataldo for analytical assistance, and Alex Zagorevski, Maurice Colpron and Discovery Helicopters (Atlin, B.C.) for field assistance. This work benefitted from critical review by N. Rayner.

## U-Pb RESULTS

**Sample:** Sandstone (ZE09079)

**GSC lab number:** z10138

**SHRIMP mount:** 582



### Zircon Description

This detrital sample is composed of clear and colourless zircon grains often displaying iron oxide staining around opaque inclusions. Grains vary from elongated to stubby prisms with sharp to sub-rounded terminations, to sub-equant zircon (above, left). Under CL (above, right), prismatic grains display broad to oscillatory zoning (grains 29 and 31), and sub-equant zircon displays oscillatory and sector zoning (grain 32).

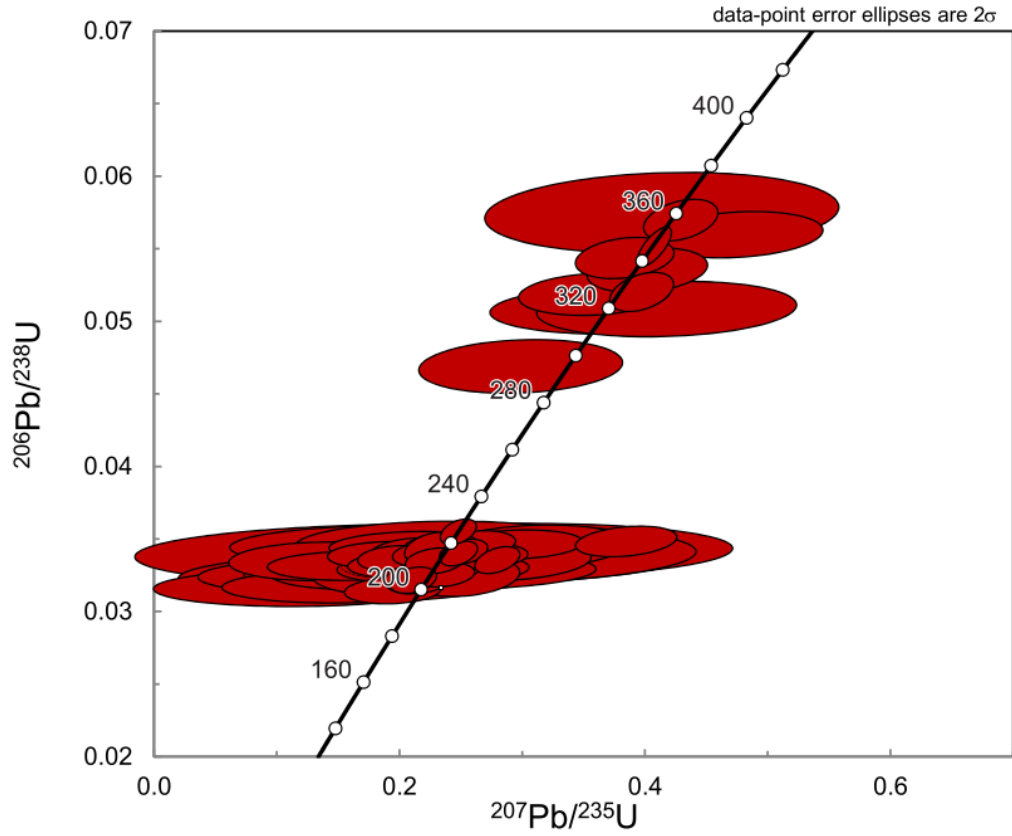
### U-Pb Results and Interpretation

A total of 70 analyses on 68 separate zircon grains were conducted. All data, including replicate analyses, are plotted in a Concordia diagram. Analyses with a probability of concordance of less than 5% are excluded, as are replicate analyses, from the probability density diagram.

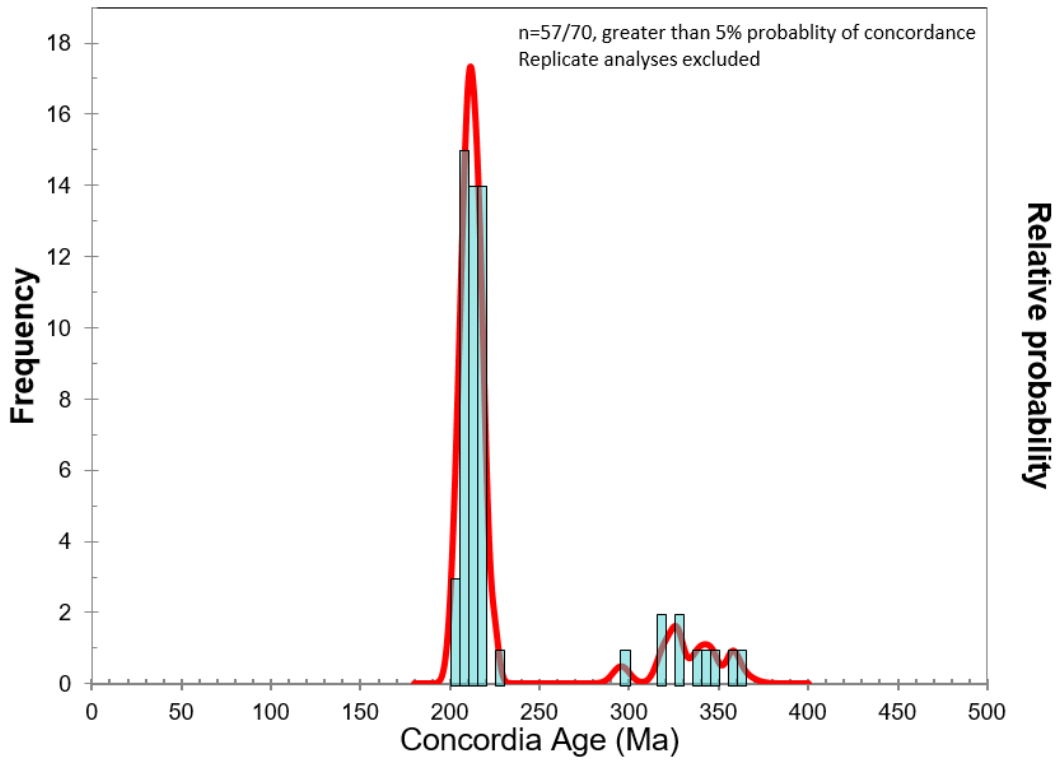
This detrital zircon population is dominated by a mode centered at ca. 210 Ma (n=49) with a subordinate population of ca. 295-360 Ma zircon (n=10). This ca. 210 Ma mode is considered the maximum age of deposition of this sandstone.



ZE09079 - z10138



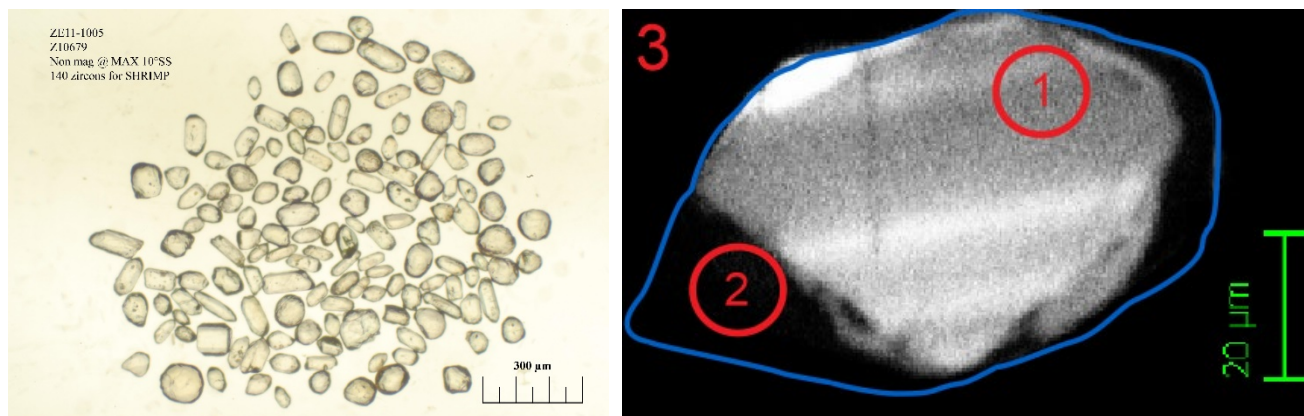
ZE09079 - z10138



**Sample:** Quartzofeldspathic schist (ZE111005)

**GSC lab number:** z10679

**SHRIMP mount:** 641



### Zircon Description

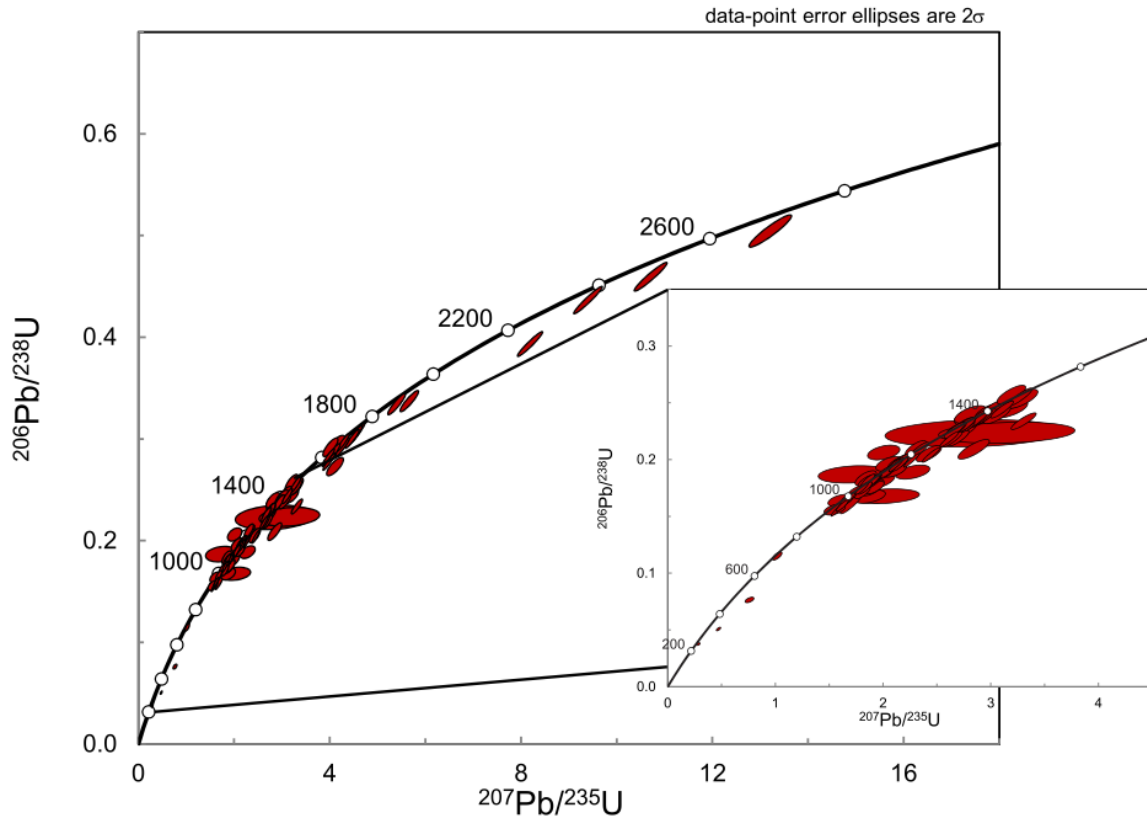
The recovered detrital zircon grains are clear and colourless with minimal inclusions. Two primary morphologies are present in this sample: equant grains and elongated prisms with sub-rounded terminations (above, left). Various modes of zoning are observed under CL, regardless of morphology. These include parallel, diffused, or broad oscillatory zoning. Zoning appears convoluted in some cases due to inclusions. Some grains exhibit weakly zoned cores surrounded by unzoned rims (e.g. grain 3, above right – grain outline in blue).

### U-Pb Results and Interpretation

A total of 92 analyses on 90 separate zircon grains were conducted. All data are plotted in a Concordia diagram. In the combined histogram/probability density diagram, all data are depicted in grey and analyses with a probability of concordance greater than 5% are depicted in red.

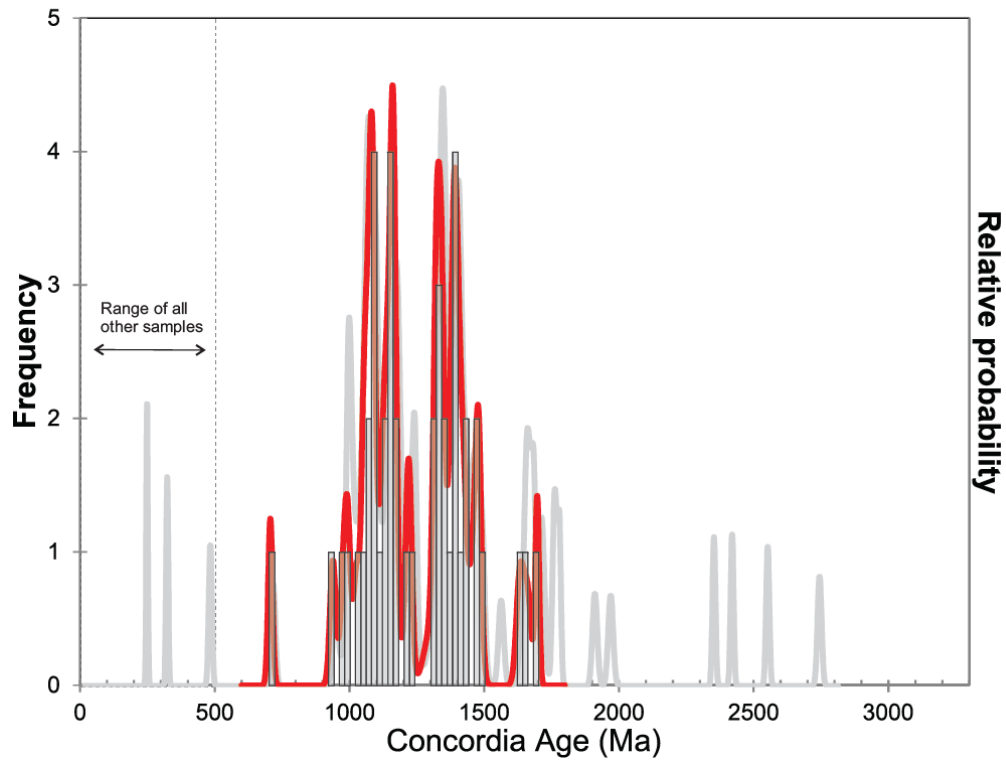
This detrital population is dominated by 2 age clusters between ca. 940-1230 Ma (n=22) and ca. 1300-1480 Ma (n=18), and subordinate clusters ranging between ca. 700-980 Ma (n=3) and ca. 1630-1700 Ma (n=3). The youngest analysis is from an overgrowth on grain 3 with a  $^{206}\text{Pb}/^{238}\text{U}$  age of  $239 \pm 3$  Ma (discordant). The age of this rim could be 239 Ma or younger, as the analysis may have nicked its ca. 1900 Ma core, and it is not clear whether it reflects pre- or post-depositional zircon growth. Thus we consider the maximum depositional age of this sample to be unconstrained.

ZE111005 - z10679



ZE111005 - z10679

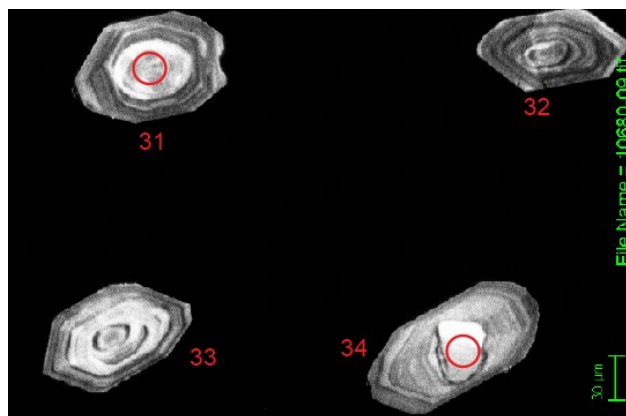
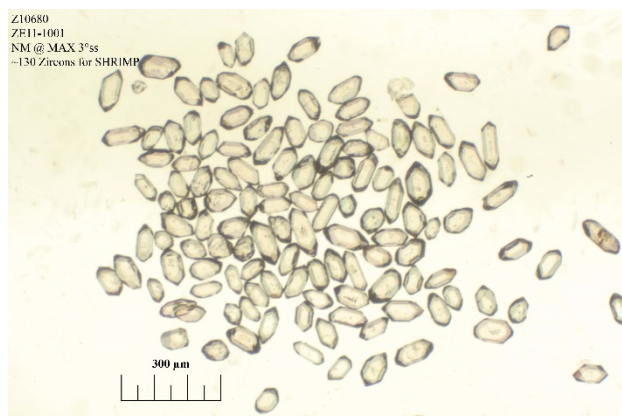
Results with greater than 5% probability of concordance shown in red (n=44/92)  
All results regardless of probability of concordance shown in grey



**Sample:** Sandstone (ZE111001)

**GSC lab number:** z10680

**SHRIMP mount:** 641



### Zircon Description

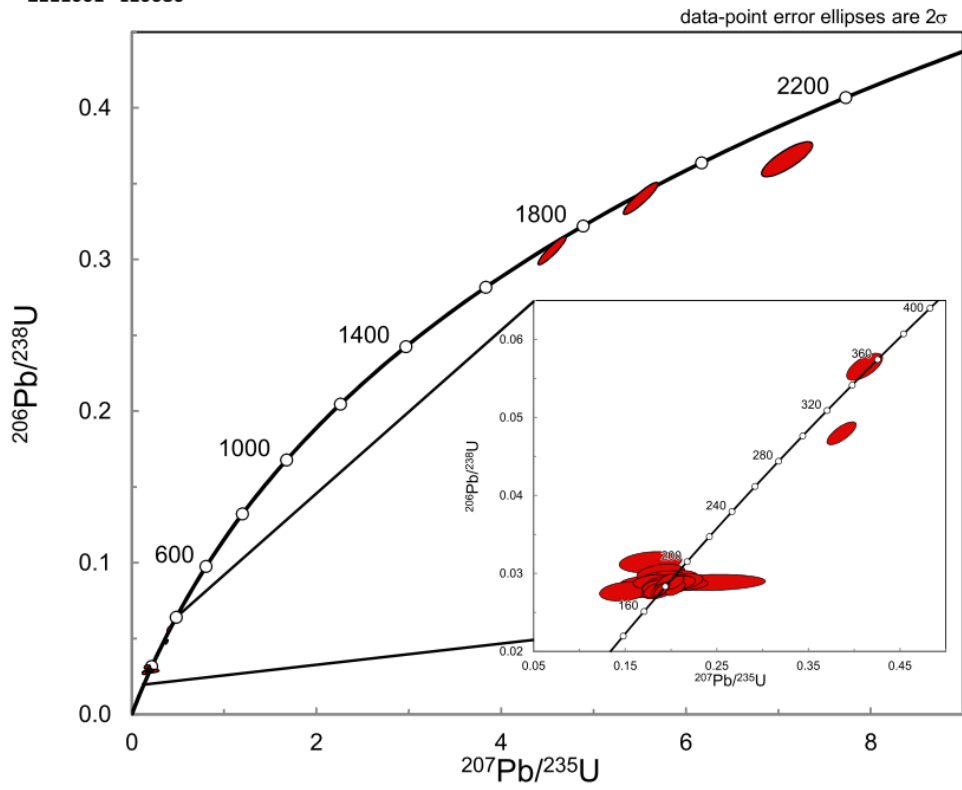
The majority of zircon grains recovered are clear and colourless prisms with sharp terminations (above, left). Some stubbier prisms with sharp to sub-rounded terminations are also present. Under CL, the majority of grains display simple oscillatory zoning and some display oscillatory-zoned rims around diffusely-zoned cores (above, right).

### U-Pb Results and Interpretation

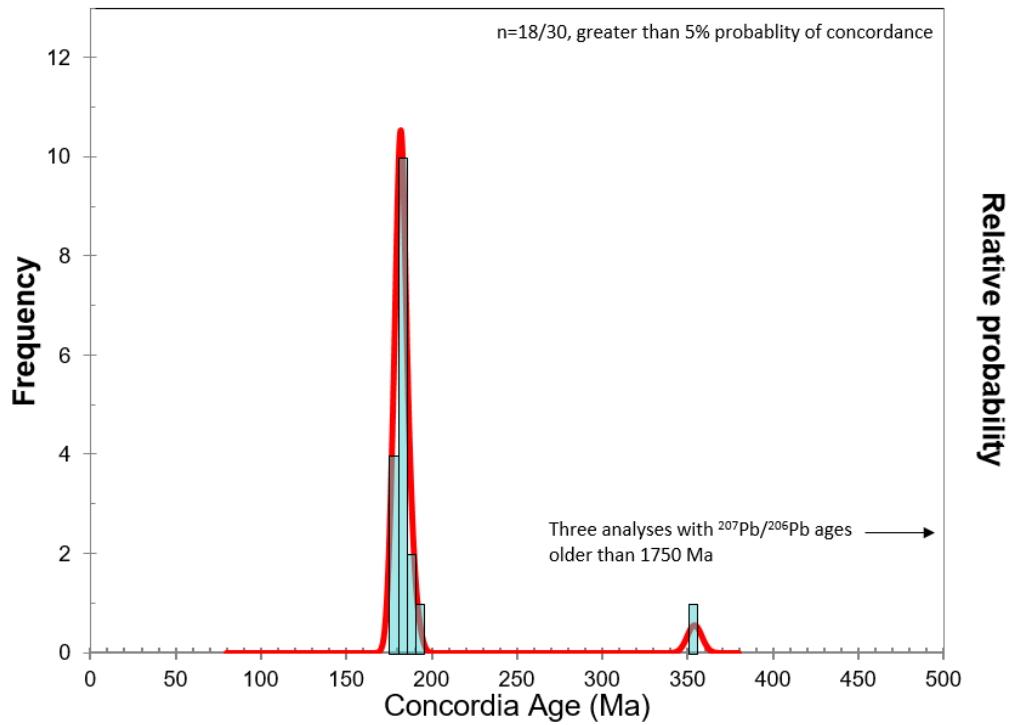
A total of 30 analyses on 30 separate grains were conducted. All data are plotted below in a Concordia diagram. Analyses with a probability of concordance less than 5% are excluded from the combined histogram/probability density diagram.

This detrital zircon population is dominated by a mode centered at ca. 183 Ma (n=18). Older detrital zircon include analyses with Concordia ages of 302 Ma (discordant) and 350 Ma (concordant), and 3 analyses of Paleoproterozoic zircon with  $^{207}\text{Pb}/^{206}\text{Pb}$  ages of ca. 1750 Ma (concordant), ca. 1910 Ma (concordant), and ca. 2160 Ma (discordant). The ca. 183 Ma mode constraints the maximum age of deposition for this sample.

Z111001 - z10680



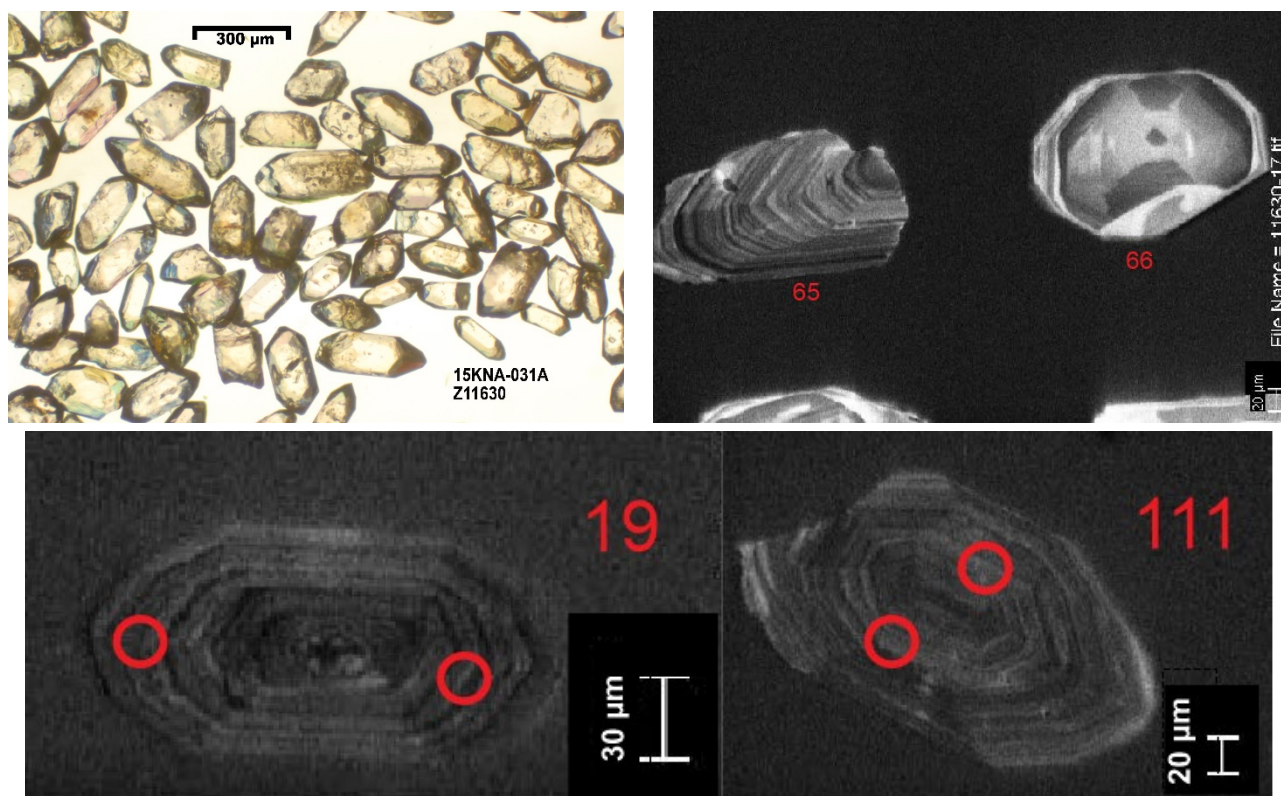
Z111001 - z10680



**Sample:** Sandstone (15-KNA-031)

**GSC lab number:** z11630

**SHRIMP mount:** 798



### Zircon Description

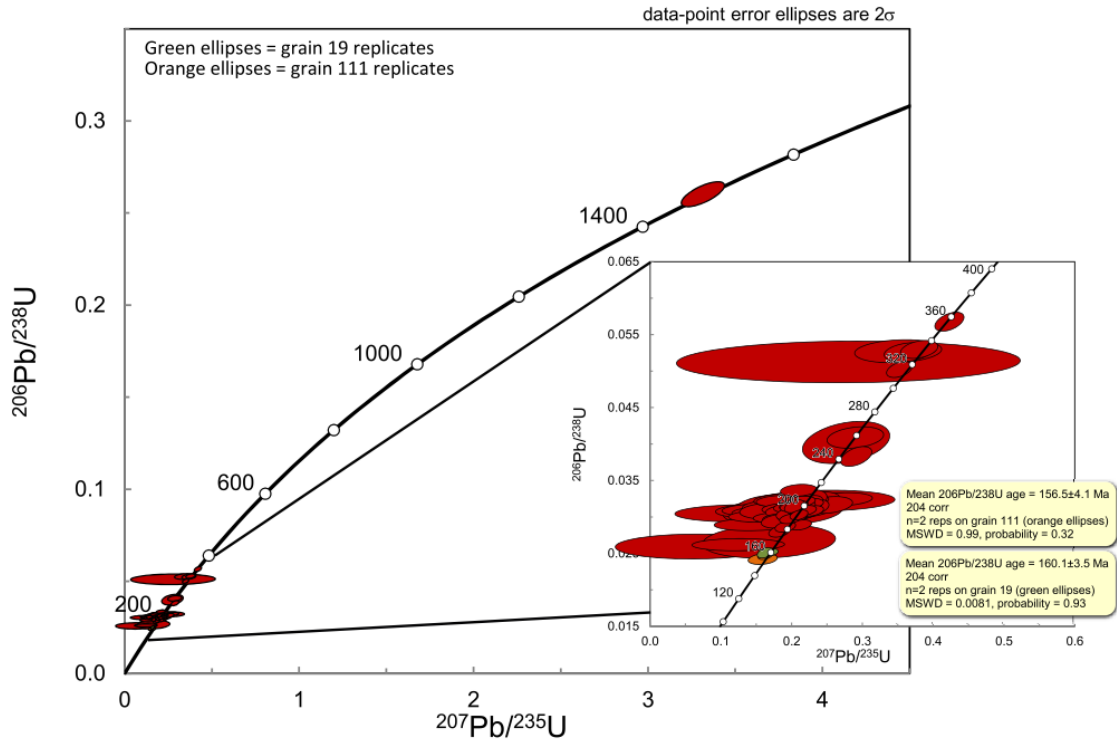
This detrital sample is composed of clear, light brown, prismatic to stubby zircon grains with sharp to sub-rounded terminations (above, top left). Under CL (above, right), grains display broadly diffuse, sector zoned cores surrounded by oscillatory zoned rims (grain 66), or are composed entirely of oscillatory zircon (grains 19, 65, and 111).

### U-Pb Results and Interpretation

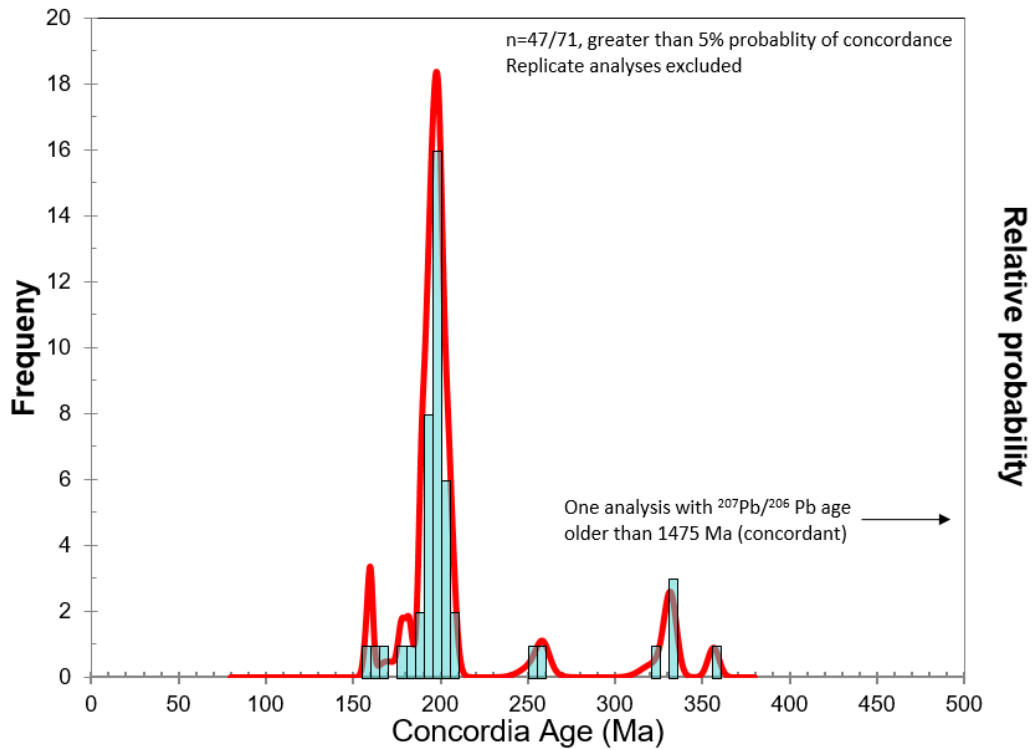
A total of 71 analyses on 67 separate grains were conducted. All data are plotted in a Concordia diagram. Analyses with a probability of concordance less than 5% are excluded from the combined histogram/probability density diagram.

This detrital zircon population is dominated by a mode centered at ca. 198 Ma composed of discrete oscillatory zoned zircon grains. Analyses on cores yield older detrital ages of ca. 260 Ma (n=2), ca. 320-355 Ma (n=5) and ca. 1475 Ma (n=1). There is also a small cluster of younger detrital oscillatory zoned zircon ranging from ca. 154-170 Ma (n=4). Replicate analyses on the two youngest detrital grains (19 and 111; discrete oscillatory zoned prisms) yield weighted  $^{206}\text{Pb}/^{238}\text{U}$  mean ages of  $160.1 \pm 3.5$  Ma (MSWD=0.081, n=2) and  $156.5 \pm 4.1$  Ma (MSWD=0.99, n=2), constraining the maximum age of deposition of this sandstone to  $156.5 \pm 4.1$  Ma.

15-KNA-031 - z11630



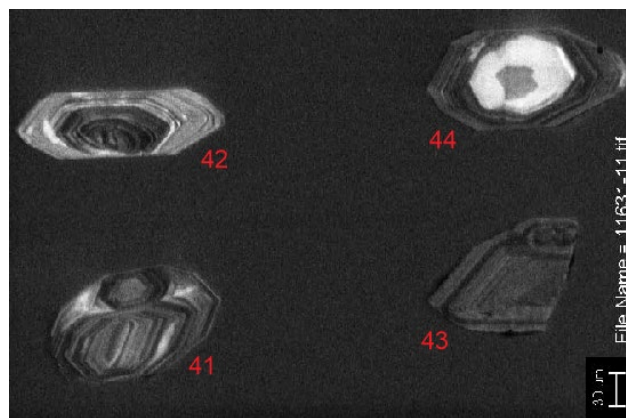
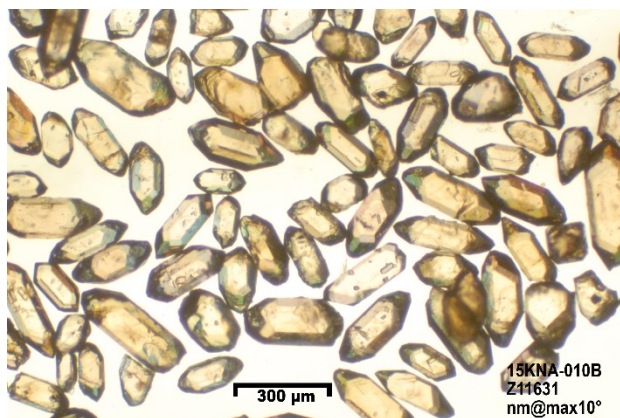
15-KNA-031 - z11630



**Sample:** Coarse-grained wacke (15-KNA-010)

**GSC lab number:** z11631

**SHRIMP mount:** 798



### Zircon Description

Zircon grains recovered from this sample are clear and light brown; the majority are elongated prisms with sharp terminations, and some grains are stubby prisms with sharp to sub-rounded terminations (above, left). Under CL, the majority of grains display simple oscillatory zoning (above, right). Some grains display a core with various modes of zonation (oscillatory, diffused, parallel, and convoluted) often disturbed by inclusions, and surrounded by an oscillatory zoned rim.

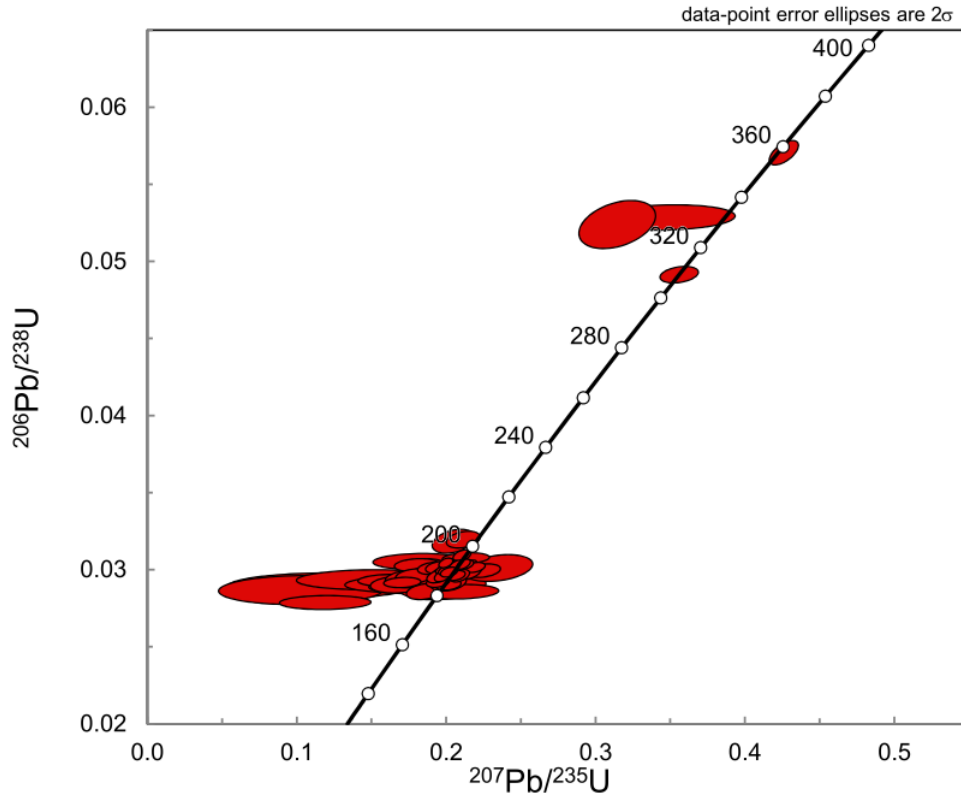
### U-Pb Results and Interpretation

A total of 64 analyses on 64 separate zircon grains were conducted. All data are plotted on a Concordia diagram. Analyses with a probability of concordance less than 5% are excluded from the combined histogram/probability density diagram.

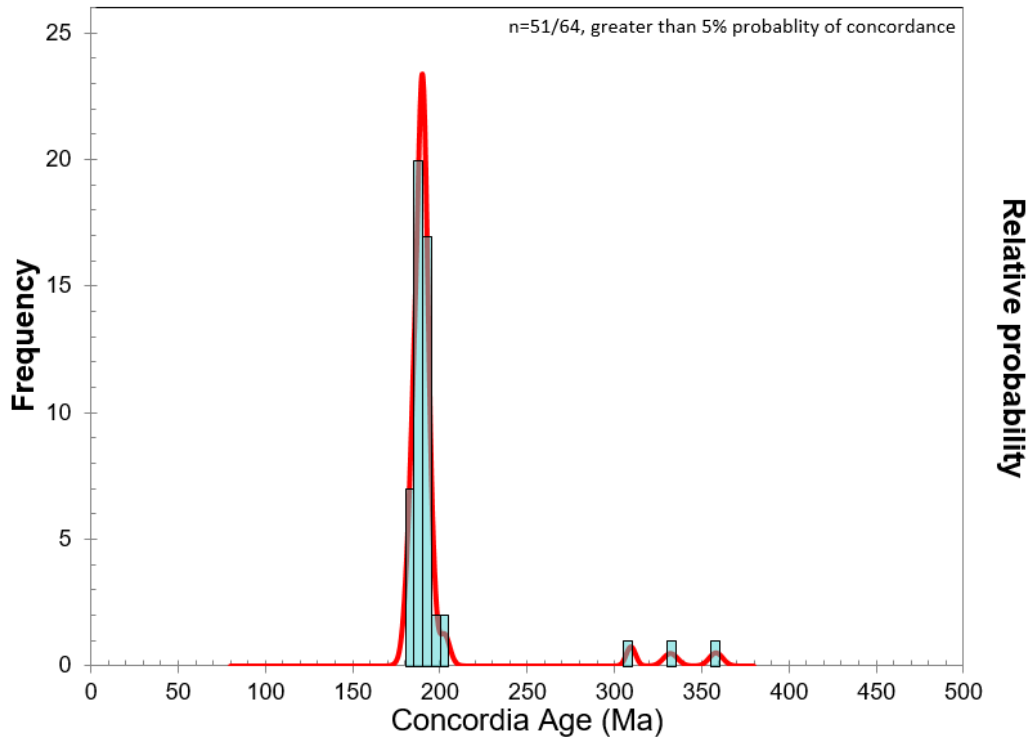
The results are characterized by a dominant mode centered at ca. 190 Ma (n=48). There are rare older detrital zircon grains with Concordia ages ranging between ca. 310-360 Ma (n=4). The ca. 190 Ma mode constrains the maximum age of deposition of this wacke.



15-KNA-010 - z11631



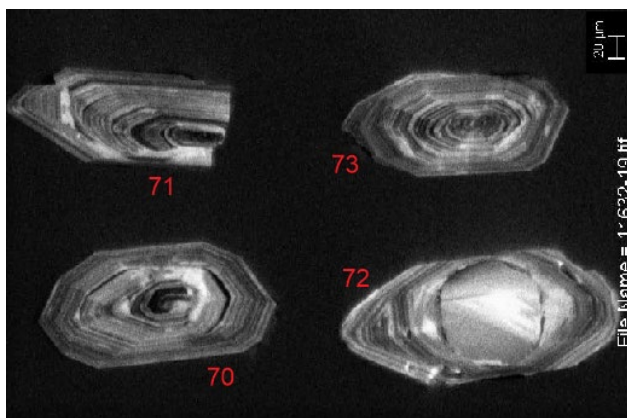
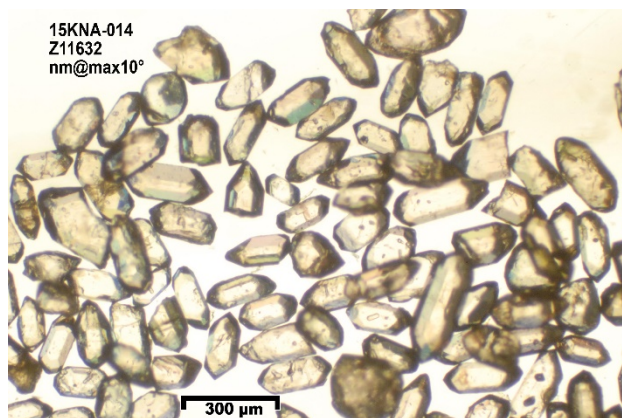
15-KNA-010 - z11631



**Sample:** Wacke (15-KNA-014)

**GSC lab number:** z11632

**SHRIMP mount:** 798



### Zircon Description

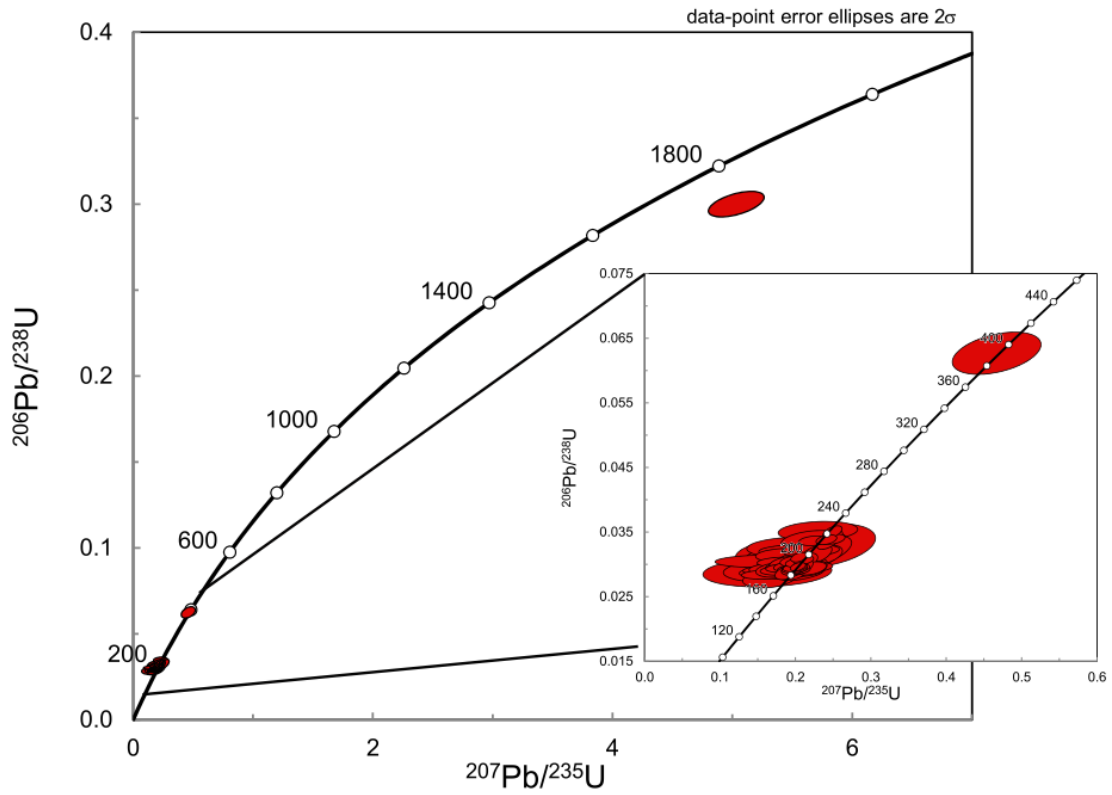
Zircon grains recovered from this sample are clear, and colourless to light brown. They are primarily prismatic with rounded to sharp terminations; sub-equant to equant grains are also common (above, left). Under CL, most (~60%) zircon grains display simple oscillatory zoning (above, right). Some (~40%) grains display a core with various zoning modes (oscillatory, diffused, parallel, and convoluted) surrounded by an oscillatory zoned rim (grain 72).

### U-Pb Results and Interpretation

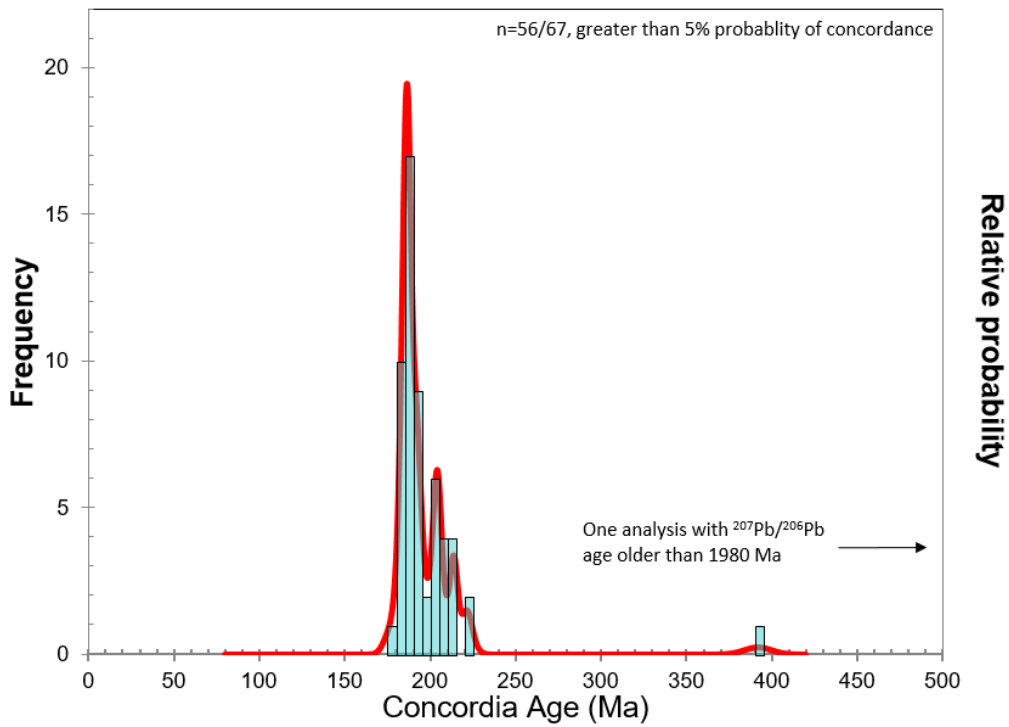
A total of 67 analyses on 67 separate zircon grains were conducted. All data are plotted on a Concordia diagram. Analyses with a probability of concordance less than 5% are excluded from the combined histogram/probability density diagram.

This detrital zircon population is dominated by a primary mode centered at ca. 187 Ma (n=38), with subordinate modes between ca. 205-230 Ma. Two analyses on cores in 2 separate zircon grains yield older results with ages of ca. 390 Ma (concordant, Concordia age) and ca. 1982 Ma (discordant,  $^{207}\text{Pb}/^{206}\text{Pb}$  age). The mode centered at ca. 187 Ma is the best estimate for the maximum age of deposition of this wacke.

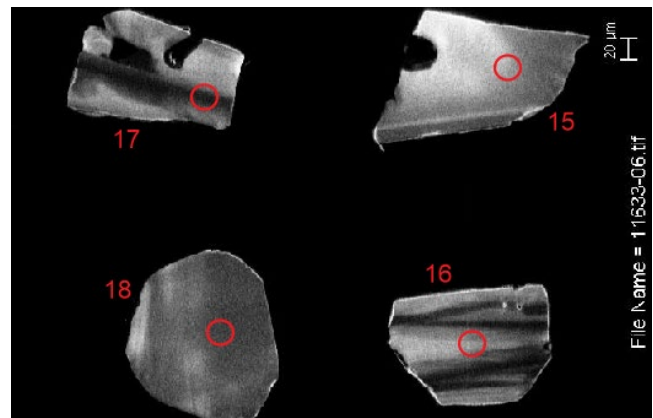
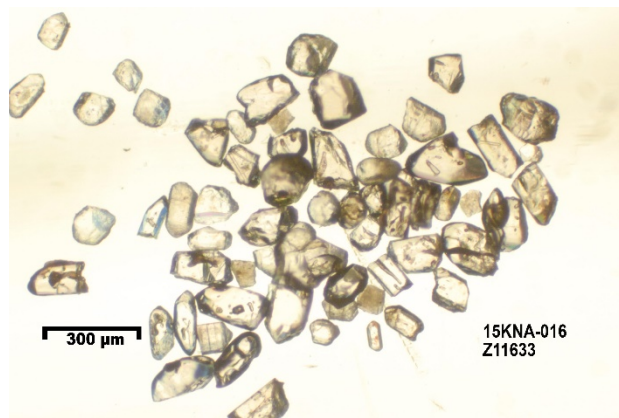
15-KNA-014 - z11632



15-KNA-014 - z11632



**Sample:** Wacke (15-KNA-016)  
**GSC lab number:** z11633  
**SHRIMP mount:** 798



### **Zircon Description**

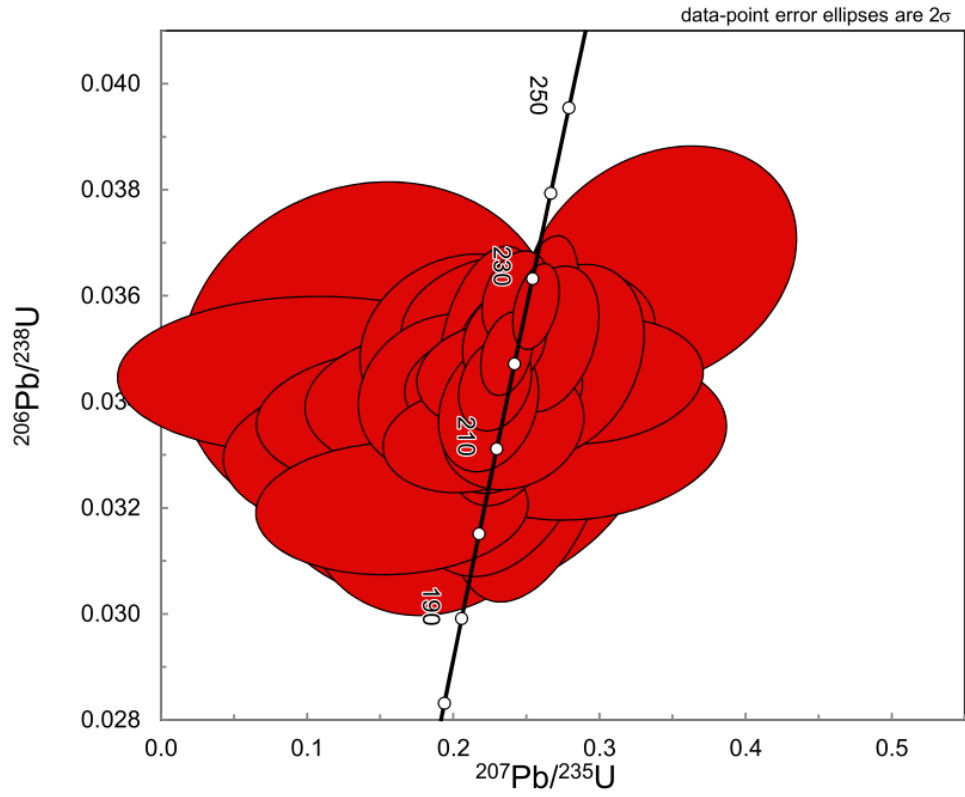
A limited number of zircon grains were recovered from this sample. They range from colourless to light brown, and are primarily anhedral fragments, with a few grains being prismatic with sub-rounded terminations (above, left). Clarity of grains varies depending on the amount of fractures. Under CL, zircon grains primarily display broad, diffuse zoning (above, right).

### **U-Pb Results and Interpretation**

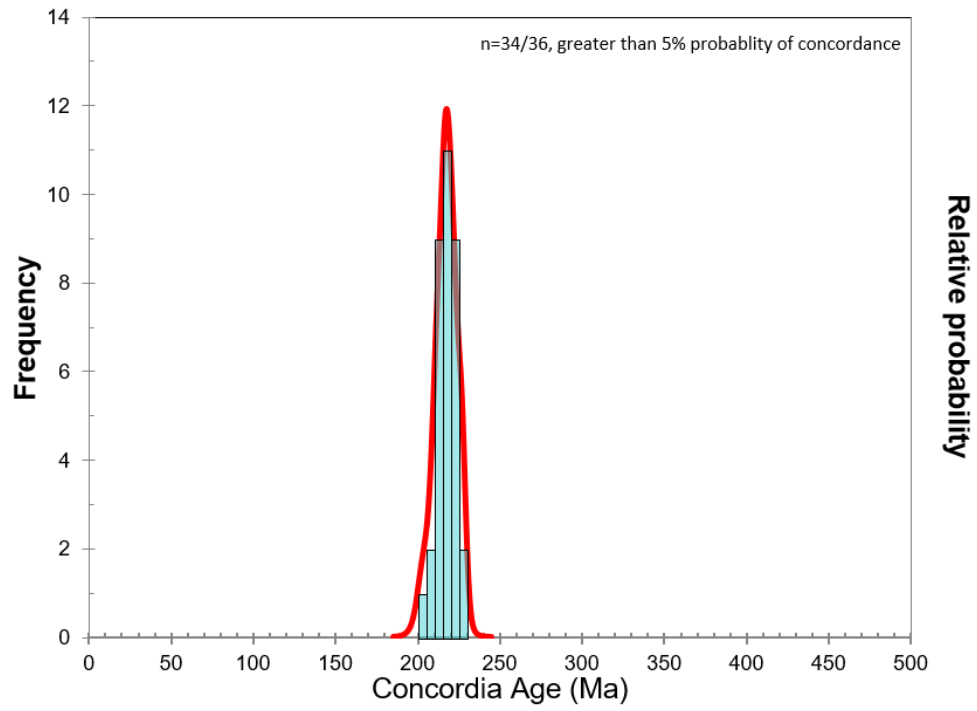
A total of 36 analyses on 36 separate zircon grains were conducted. All data are plotted on a Concordia diagram. Analyses with a probability of concordance less than 5% are excluded from the combined histogram/probability density diagram.

This detrital zircon population forms a unimodal distribution centered at ca. 218 Ma (n=34), constraining the maximum age of deposition of this wacke.

15-KNA-06 - z11633



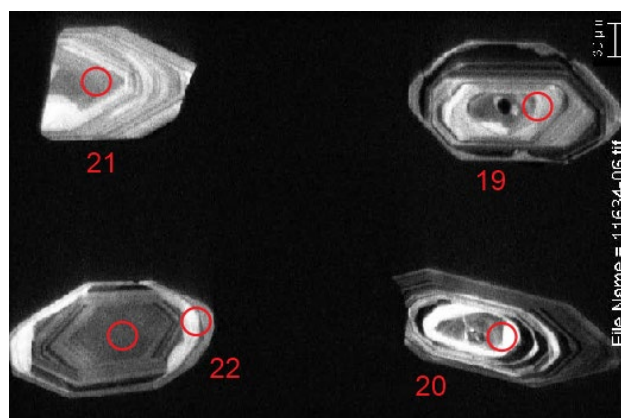
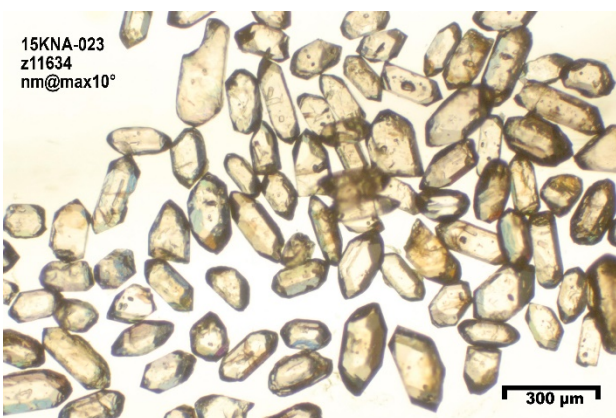
15-KNA-016 - z11633



**Sample:** Coarse sandstone/wacke (15-KNA-023)

**GSC lab number:** z11634

**SHRIMP mount:** 798



### Zircon Description

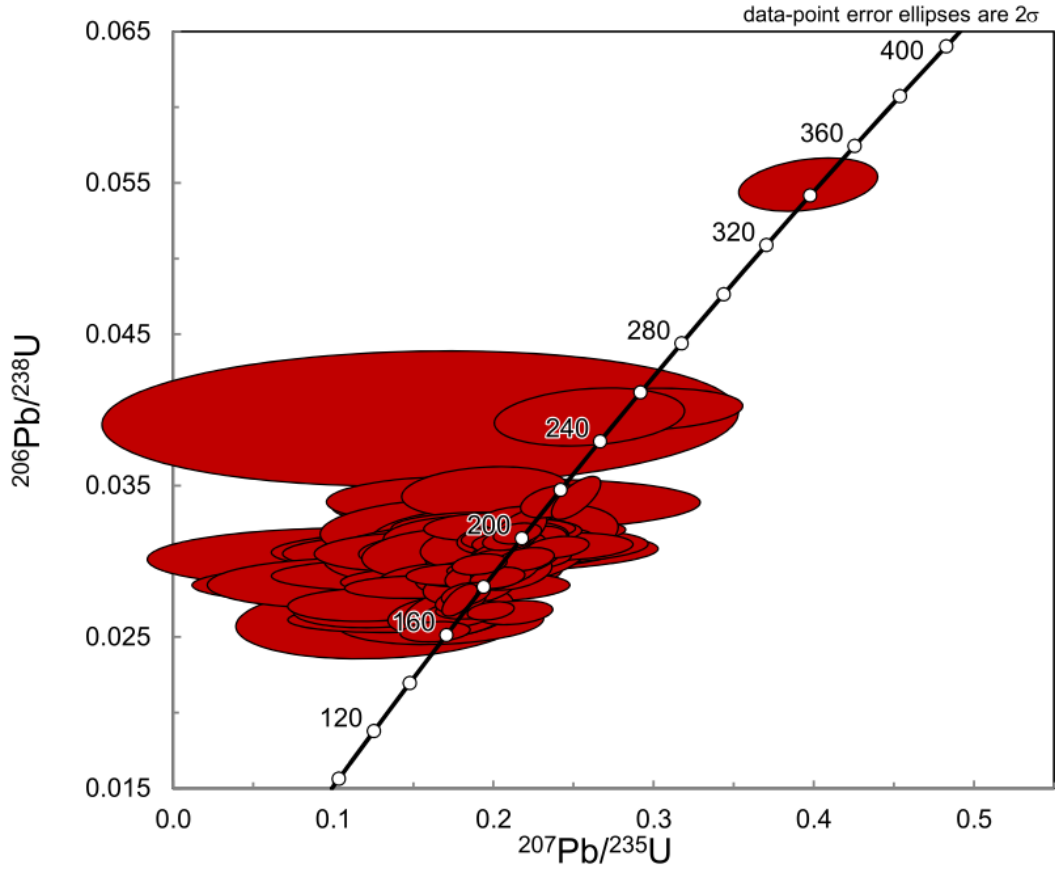
Zircon grains recovered from this sample are clear and colourless. The majority of the grains are prismatic with sharp to rounded terminations; some stubbier grains are also present (above, left). Under CL, zircon grains primarily display simple oscillatory zoning. Some grains are composed of a subhedral to anhedral core surrounded by an oscillatory zoned rim. A thin 5-10 μm unzoned rim is observed in a few grains (grain 22, above right).

### U-Pb Results and Interpretation

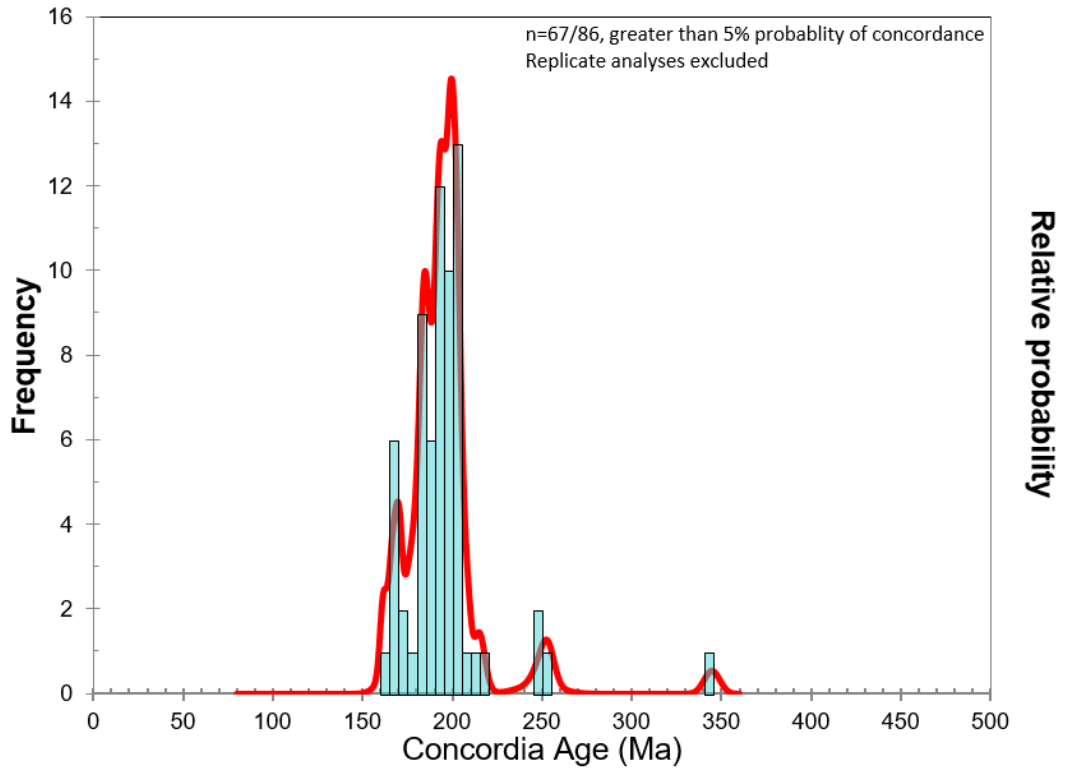
A total of 86 analyses on 83 separate zircon grains were conducted. All data are plotted on a Concordia diagram. Analyses with a probability of concordance less than 5% are excluded from the combined histogram/probability density diagram.

Eighty-two of these analyses yield concordant ages between 160-220 Ma, with a primary mode at ca. 200 Ma and subordinate modes at ca. 185 Ma and ca. 170 Ma; these occur in either oscillatory zoned rims or discrete oscillatory zoned grains. The cores of older detrital zircon grains yield Concordia ages of ca. 250 Ma (n=3) and ca. 350 Ma (n=1). The youngest subordinate mode of ca. 170 Ma is comprised of 14 analyses ranging between 160-174 Ma; these analyses occur in oscillatory zoned areas of prismatic zircon grains, and thus reflect detrital ages rather than metamorphic overgrowths. This population at ca. 170 Ma is interpreted to constrain the maximum age of deposition of this sandstone.

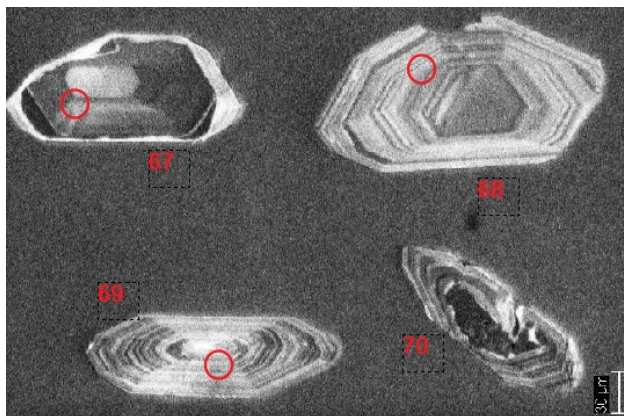
15-KNA-023 - z11634



15-KNA-023 - z11634



**Sample:** Sandstone/wacke with garnet clasts (15-KNA-005)  
**GSC lab number:** z12357  
**SHRIMP mount:** 922



### Zircon Description

Zircon grains recovered from this detrital sample are primarily prismatic with sharp to sub-rounded terminations; a few stubbier sub-equant grains were also recovered. Under CL, zircon grains display oscillatory zoning; some are simple oscillatory zoned grains (grain 69) and some contain anhedral to euhedral cores surrounded by an oscillatory zoned rim (grains 67 and 70). The cores contain either oscillatory, broad or convoluted zoning due to inclusions.

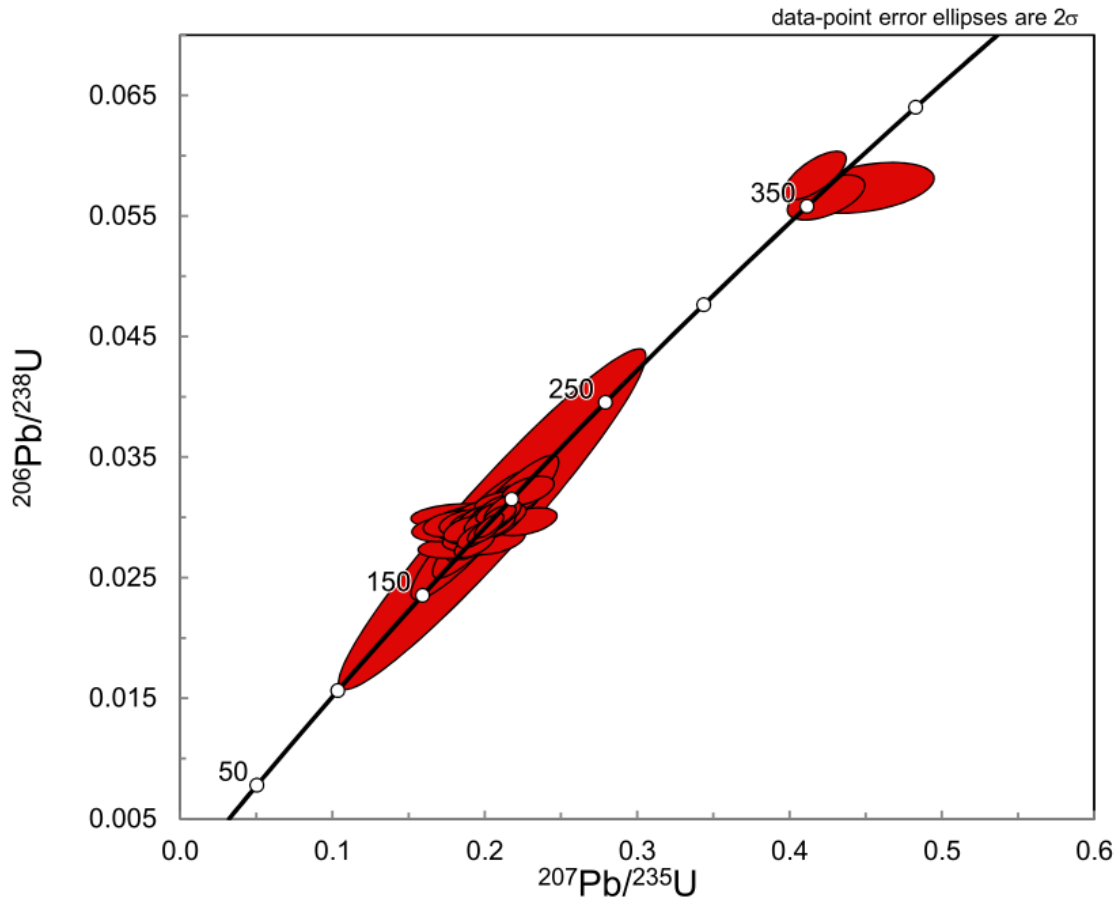
### U-Pb Results and Interpretation

A total of 66 analyses on 63 separate zircon grains were conducted. Data are plotted on two separate Concordia diagrams; one includes all data analyses and a more detailed one focuses on replicate analyses. Analyses with a probability of concordance less than 5% are excluded, as are replicate analyses, from the combined histogram/probability density diagram.

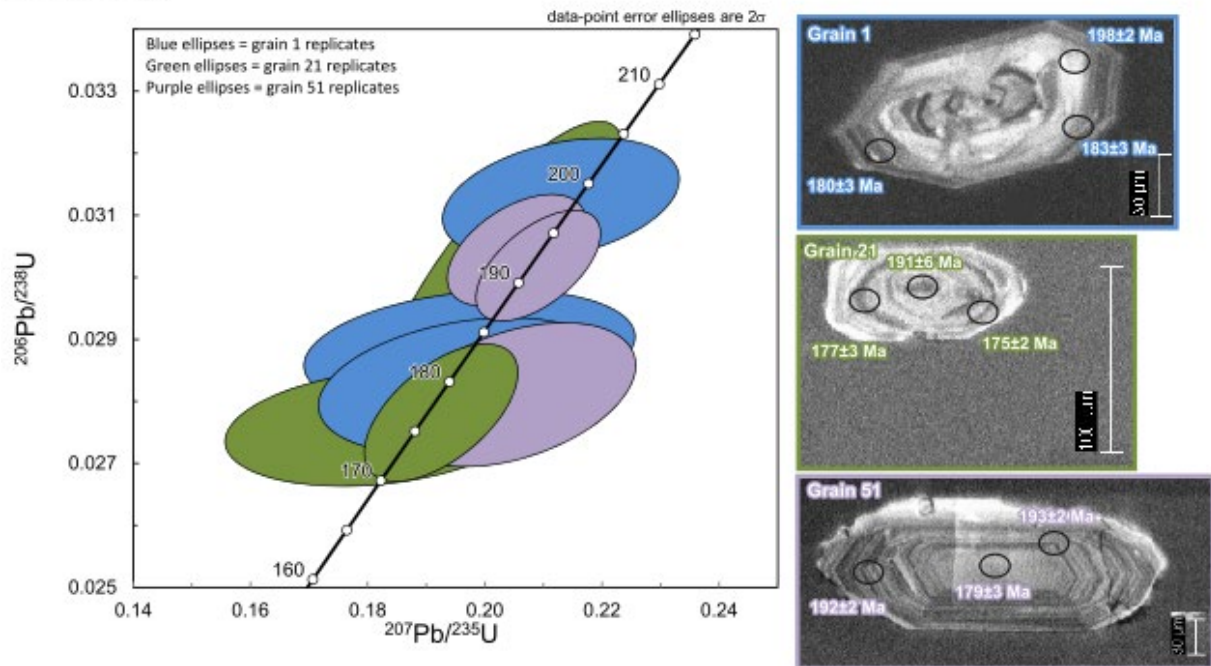
The majority of data for this detrital sample yields concordant ages between 175-205 Ma, displaying a unimodal distribution at ca. 190 Ma (n=28). A subordinate mode composed of 3 concordant analyses on 3 separate grains occurs at 360 Ma. Two replicate analyses on the outer oscillatory zoned portion of grain 21, give a  $^{206}\text{Pb}/^{238}\text{U}$  age of  $176.0 \pm 3.6$  (MSWD=0.17); a single analysis on the inner portion of this grain yields an age of  $191 \pm 6$  Ma. Replicate analyses on two additional young detrital grains (grains 1 and 51) yielded inconsistent results as observed in the detailed Concordia diagram. Due to reproducibility issues exhibited on these replicate analyses, we interpret the mode at ca. 190 Ma to best represent the maximum depositional age.



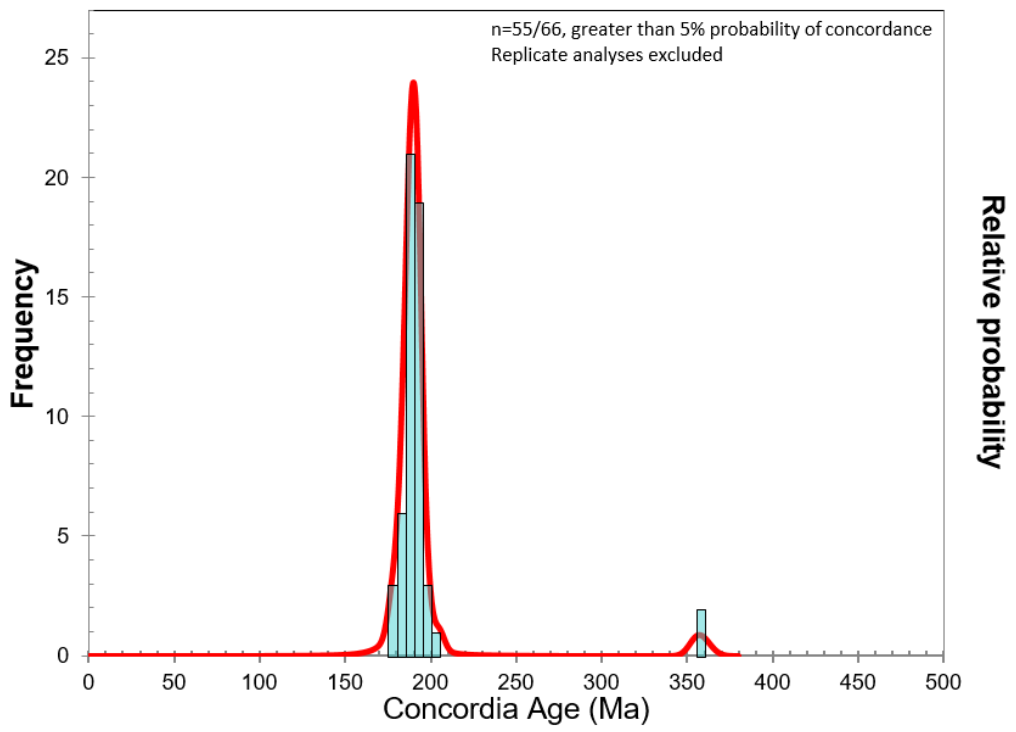
15-KNA-005 - z12357



15-KNA-005 - z12357



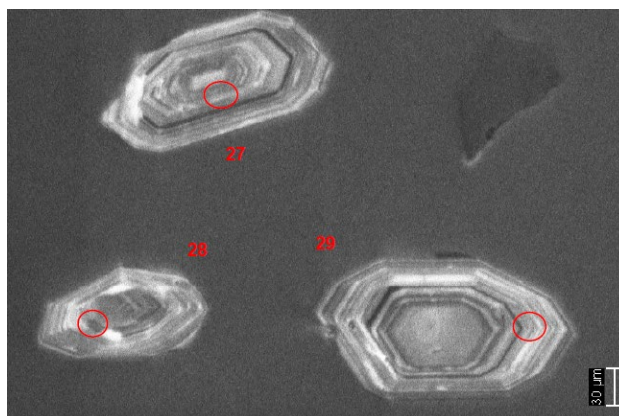
15-KNA-005 - z12357



**Sample:** Fine-grained sandstone with mudstone rip-ups (15-KNA-030)

**GSC lab number:** z12358

**SHRIMP mount:** 922



### **Zircon Description**

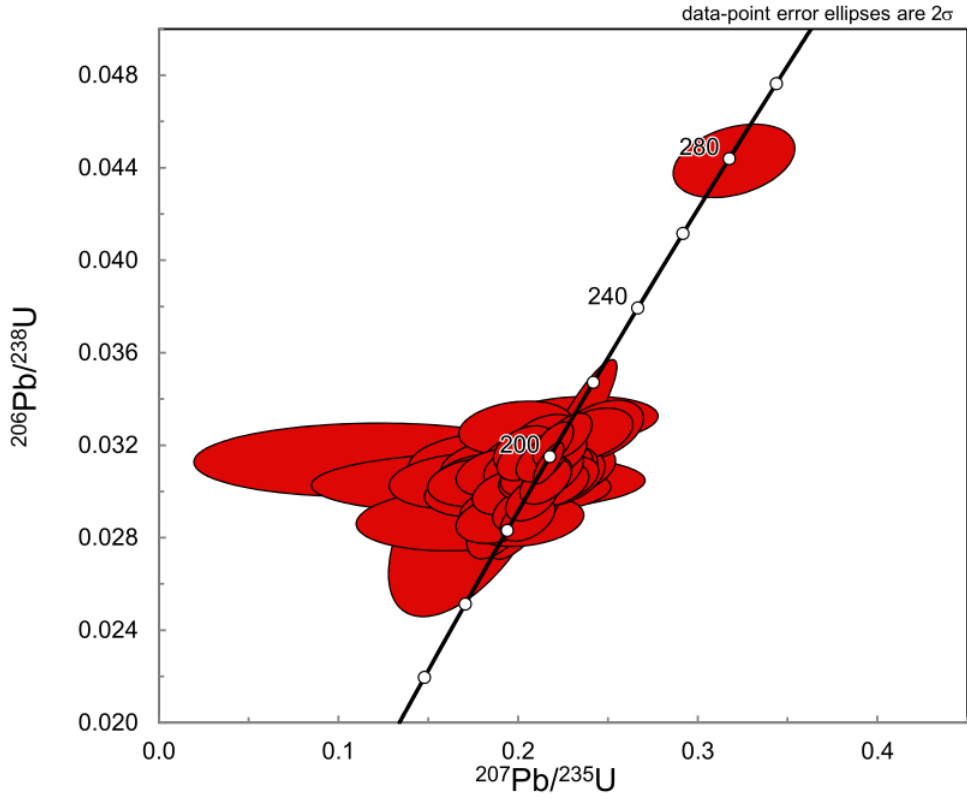
Zircon grains recovered from this detrital sample range from stubby (primarily) to elongated prisms with sharp to sub-rounded terminations. Under CL, zircon grains either display discrete oscillatory zoning, or an oscillatory-zoned rim on a euhedral, oscillatory-zoned, broadly-zoned or unzoned core.

### **U-Pb Results and Interpretation**

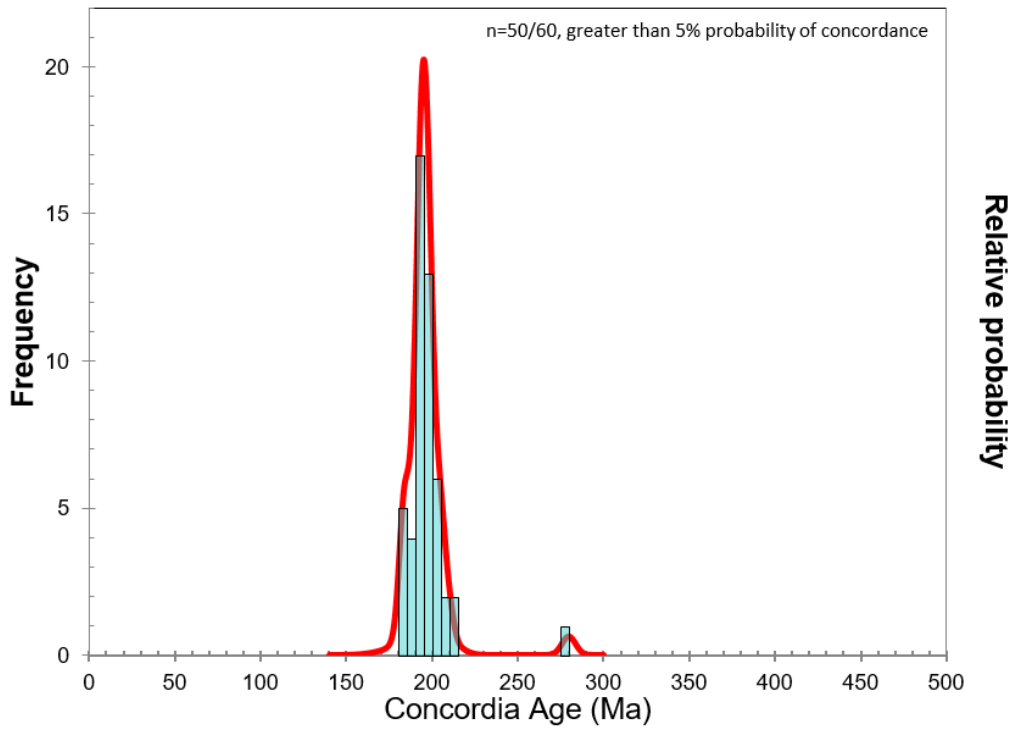
A total of 60 analyses on 60 separate grains were conducted. All data are plotted on a Concordia diagram. Analyses with a probability of concordance less than 5% are excluded from the combined histogram/probability density diagram.

This detrital zircon population is characterized by a dominant mode centered between ca. 190-200 Ma. A single analysis on a core (grain 21) yields an older Concordia age of ca. 280 Ma (concordant). Skewness in the ca. 190-200 Ma mode to younger ages is caused by 7 younger concordant analyses between ca. 181-186 Ma. Ludwig's (2003) unmix function in Isoplot v. 4.15 separates analyses into two components at  $201.1 \pm 2.3$  Ma and  $191.5 \pm 1.5$  Ma (relative misfit = 0.801). As the calculated error of the youngest age falls below the long term precision threshold, this result is more appropriately reported as  $191.5 \pm 1.9$  Ma, interpreted as the maximum deposition age of this sandstone.

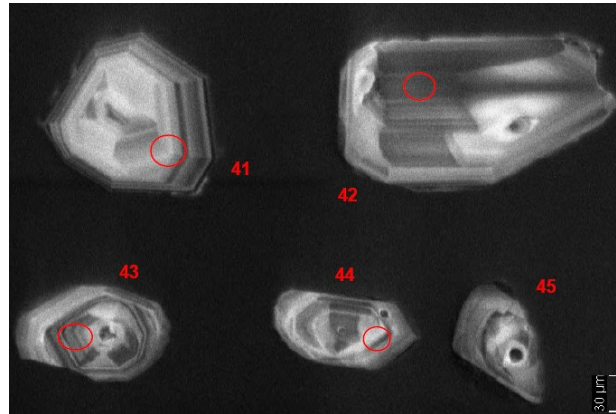
15-KNA-030 - z12358



15-KNA-030 - z12358



**Sample:** Conglomerate (15-KNA-035)  
**GSC lab number:** z12359  
**SHRIMP mount:** 922



### **Zircon Description**

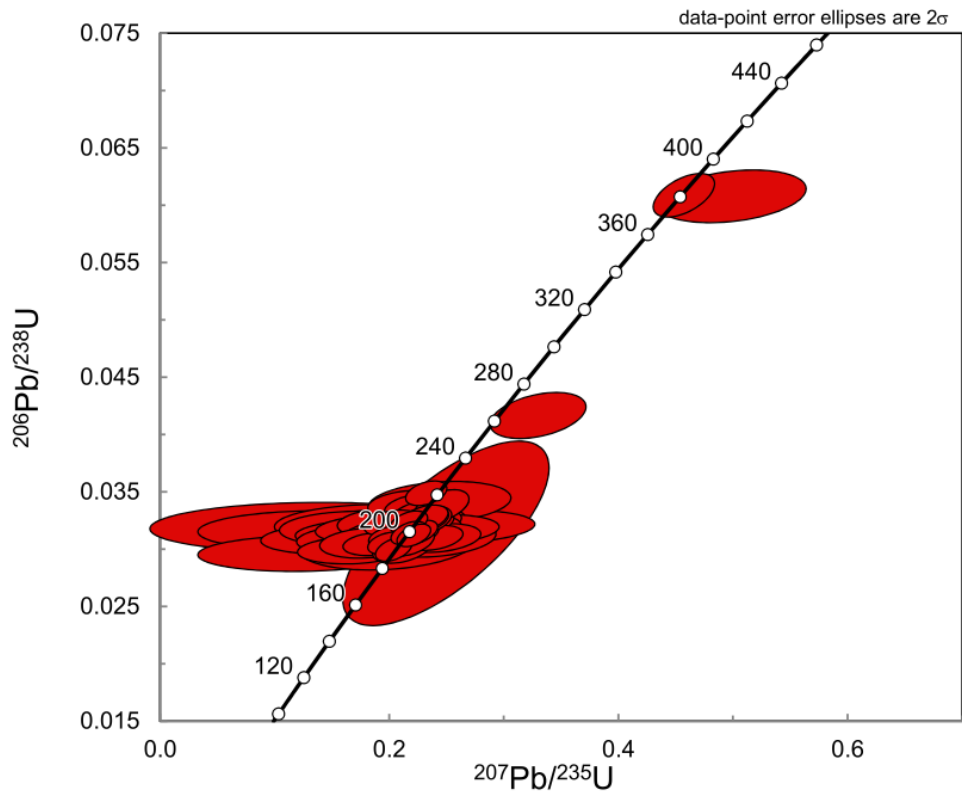
Zircon grains recovered from this conglomerate range from prisms with sharp to sub-rounded terminations, to anhedral fragments. Under CL, most grains contain inner areas ranging in size and zoning type (diffused, sector, and oscillatory zoning), surrounded by oscillatory zoned outer areas of various thickness; the prominence of zoning in outer areas varies between grains. Some inclusions are present, and various degrees of fracturing are observed between grains.

### **U-Pb Results and Interpretation**

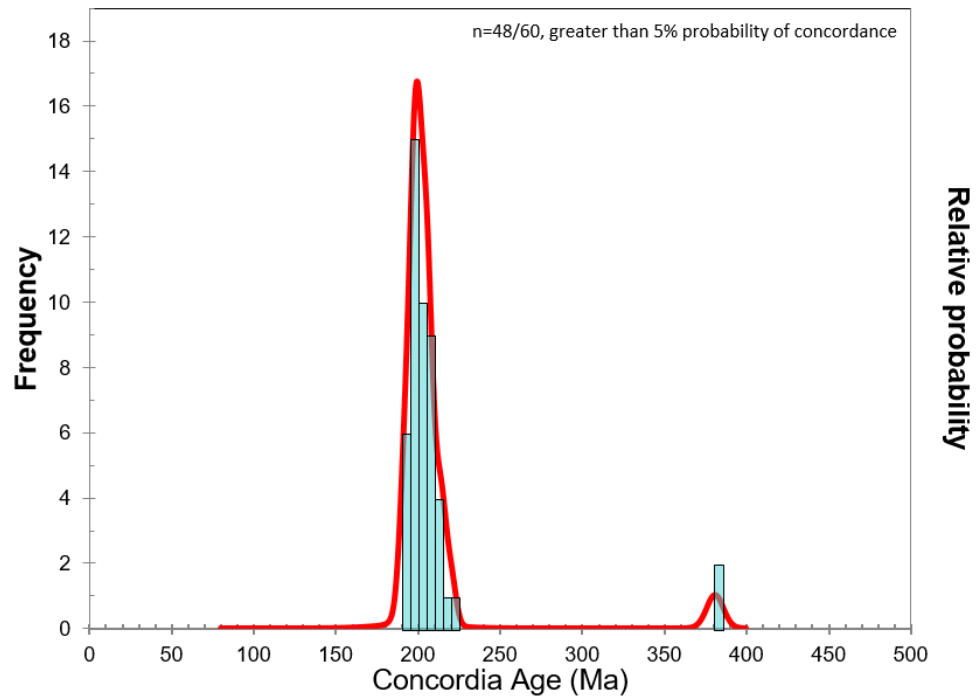
A total of 60 analyses on 60 separate grains were conducted. All data are plotted on a Concordia diagram. Analyses with a probability of concordance less than 5% are excluded from the combined histogram/probability density diagram.

This detrital zircon population is characterized by a dominant mode at ca. 200 Ma (n=46), with Concordia ages ranging between ca. 188-260 Ma; no age difference is observed between inner and outer zoned areas of grains. Older detrital zircon grains yield Concordia ages of ca. 380 Ma (n=2; concordant). The ca. 200 Ma mode is the best estimate for the maximum age of deposition of this conglomerate.

15-KNA-035 - z12359



15-KNA-035 - z12359



## <sup>40</sup>Ar/<sup>39</sup>Ar RESULTS

**Sample:** Quartz-mica schist cobble in conglomerate (15-KNA-021B)

**GSC lab number:** z11628

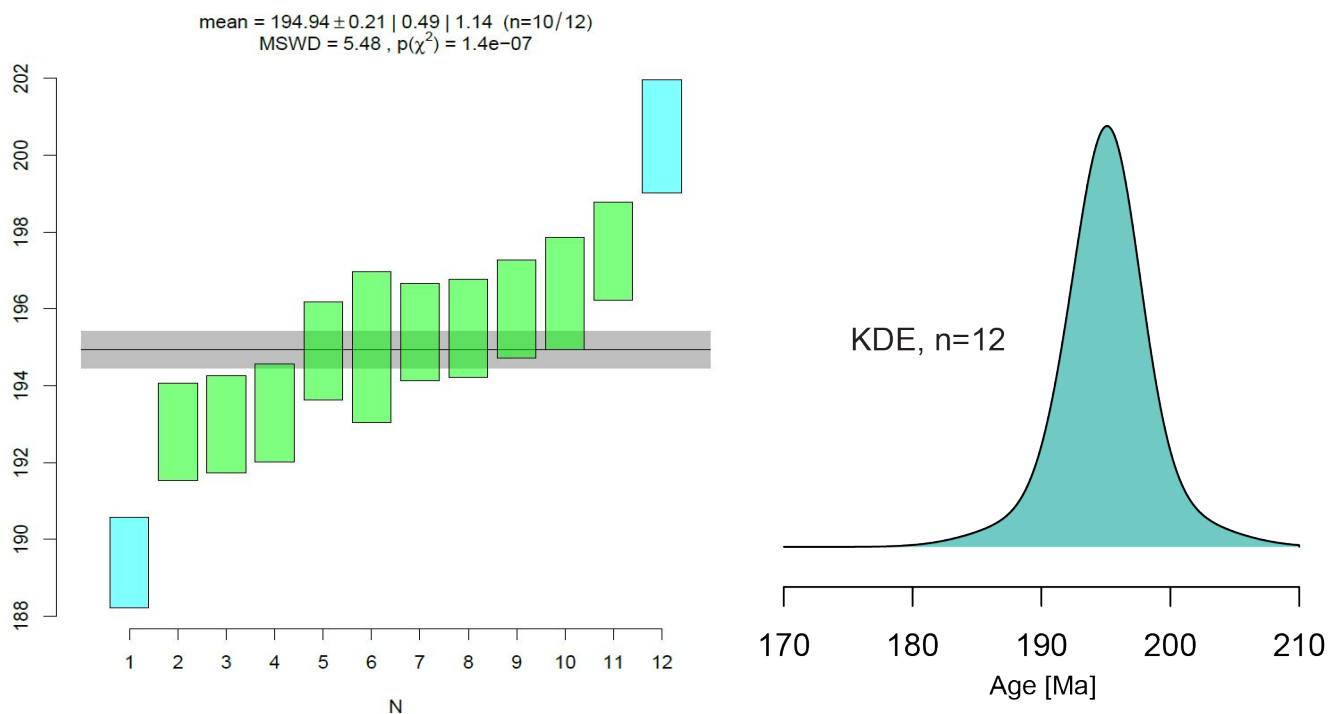
**Ar#:** 3553

### Summary of single crystal step heating results:

Aliquot/Grain	Age (Ma)	2σ error (Ma)	Age type	MSWD	steps	% <sup>39</sup> Ar released
1	197.5	1.3	Integrated			
2	193.3	1.3	Plateau	0.24	C-H, n=6	96.8
3	193.0	1.3	Plateau	0.45	D-I, n=6	98.8
4	196.0	1.3	Integrated			
5	194.9	1.3	Integrated			
6	200.5	1.5	Integrated			
7	196.4	1.5	Plateau	1.52	A-D, n=3	92.3
8	195.0	2	Plateau	2.64	D-H, n=4	72.7
9	192.8	1.3	Plateau	0.05	M-O, n=3	76.4
10	195.5	1.3	Plateau	0.45	E-G, n=3	64.1
11	195.4	1.3	Plateau	2.51	C-F, n=4	65.0
12	189.4	1.2	Plateau	0.85	I-M, n=5	49.9

### <sup>40</sup>Ar/<sup>39</sup>Ar Interpretation

The single crystal step heat ages obtained from this detrital metamorphic cobble yield a weighted mean age of  $195 \pm 1$  Ma ( $n=10/12$ , MSWD=5.5, error estimated at 0.5% based on reproducibility of secondary standard), as well as a single mode centered at 195 Ma in a kernel density estimate (KDE) plot (IsoplotR; Vermeesch, 2018). These results indicate both a maximum depositional age for the conglomerate of 195 Ma, as well as a cooling age through  $\sim 400$  °C (nominal closure temperature for muscovite) for the source quartz-mica schist.



Sample: Sandstone (15-KNA-034)

GSC lab number: z11629

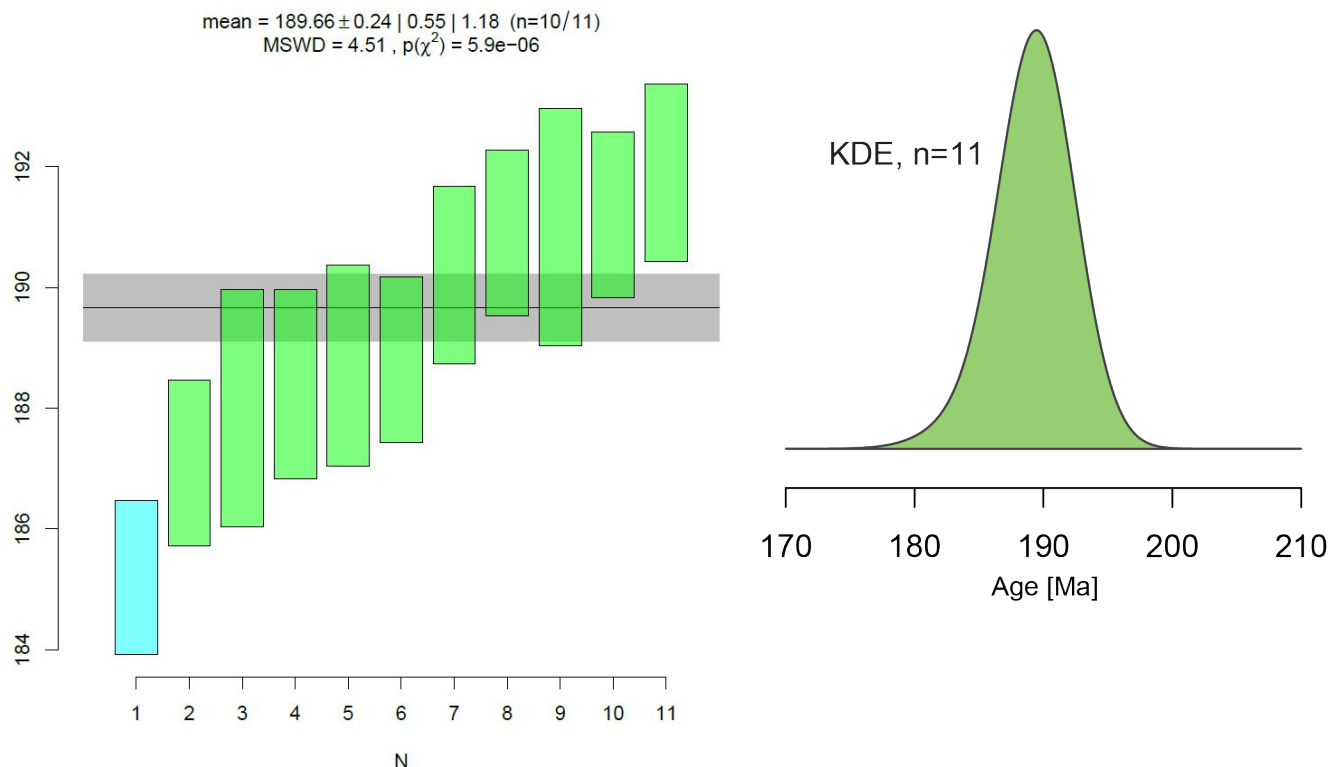
Ar#: 3554

**Summary of single crystal step heating results:**

Aliquot/Grain	Age (Ma)	2σ error (Ma)	Age type	MSWD	steps	% <sup>39</sup> Ar released
1	188.0	2	Plateau	0.87	B-I, n=8	93.5
2	191.2	1.4	Plateau	1.20	C-L, n=10	90.4
3	185.2	1.3	Plateau	1.05	B-H, n=7	93.9
4	188.7	1.7	Plateau	0.67	A-D, n=4	100.0
5	188.4	1.6	Plateau	0.37	B-E, n=4	76.3
6	187.1	1.4	Plateau	1.25	B-G, n=4	66.4
7	188.8	1.4	Plateau	1.37	B-H, n=7	92.1
8	190.2	1.5	Plateau	0.62	B-H, n=7	90.0
9	191.0	2	Plateau	1.44	A-F, n=5	69.4
10	191.9	1.5	Plateau	1.31	A-H, n=6	100.0
11	190.9	1.4	Pseudo-plateau			

**<sup>40</sup>Ar/<sup>39</sup>Ar Interpretation**

The single crystal ages obtained for 11 detrital muscovite grains from this sandstone yield a kernel density estimate with a single mode at 190 Ma (IsoplotR). The weighted mean age of the detrital grains is 190±1 Ma (n=10/11, MSWD=4.5, error estimated at 0.5% based on reproducibility of secondary standard). The high MSWD of the sample may indicate a subtle range in source muscovite cooling ages. These results indicate both a maximum depositional age for the sandstone of 190 Ma, as well as a cooling age through ~400 °C (nominal closure temperature for muscovite) for the muscovite-containing source rock(s).





## REFERENCES

- Black, L.P., Kamo, S.L., Allen, C.M., Davis, D.W., Aleinikoff, J.N., Valley, J.W., Mundil, R., Campbell, I.H., Korsh, R.J., Williams, I.S., Foudoulis, C., 2004. Improved  $^{206}\text{Pb}/^{238}\text{U}$  microprobe geochronology by monitoring of a trace-element-related matrix effect; SHRIMP, ID-TIMS, ELA-ICP-MS and oxygen isotope documentation for a series of zircon standards: *Chemical Geology*, 205, 115-140.
- Colpron, M., Crowley, J.L., Gehrels, G., Long, D.G.F., Murphy, D.C., Beranek, L., and Bickerton, L., 2015. Birth of the northern Cordilleran orogen, as recorded by detrital zircons in Jurassic synorogenic strata and regional exhumation in Yukon. *Lithosphere*, 7, 541-562.
- Colpron, M., Israel, S., Murphy, D., Pigage, L. and Moynihan, D., 2016. Yukon Bedrock Geology Map. Yukon Geological Survey, Open File 2016-1, 1: 1,000,000 scale map and legend.
- Coney, P.J., Jones, D.L., and Monger, J.W.H., 1980. Cordilleran suspect terranes. *Nature (London)*, 288, 329-333.
- Cui, Y., Miller, D., Schiarizza, P., and Diakow, L.J., 2017. British Columbia digital geology. British Columbia Ministry of Energy, Mines and Petroleum Resources, British Columbia Geological Survey Open File 2017-8, 9p. Data version 2018-04-05.
- Deino, A.L., 2001. User's manual for Mass Spec v. 5.02. Berkeley Geochronology Center Special Publication 1a, Berkeley Geochronology Center, Berkeley California, 119 p.
- Dickinson, W.R. and Gehrels, G.E., 2009. Use of U–Pb ages of detrital zircons to infer maximum depositional ages of strata: a test against a Colorado Plateau Mesozoic database. *Earth and Planetary Science Letters*, 288, 115-125.
- English, J.M., Johannson, G.G., Johnston, S.T., Mihalyuk, M.G., Fowler, M., and Wight, K.L., 2005. Structure, stratigraphy and petroleum resource potential of the Central Whitehorse Trough, Northern Canadian Cordillera. *Bulletin of Canadian Petroleum Geology*, 53, 130-153.
- Evenchick, C A; Thorkelson, D J., 2005. Geology of the Spatsizi River map area, north-central British Columbia; Geological Survey of Canada, Bulletin no. 577, 276 p.; 1 CD-ROM, <https://doi.org/10.4095/215877>.
- Hutchison, M.P., 2017. Whitehorse trough: Past, present and future petroleum research – with a focus on reservoir characterization of the northern Laberge Group. Yukon Geological Survey, Open File 2017-2, 48 p. plus appendices and plates.
- Johannson, G.G., Smith, P.L., Gordey, S.P., 1997. Early Jurassic evolution of the northern Stikinian arc: evidence from the Laberge Group, northwestern British Columbia. *Canadian Journal of Earth Sciences*, 34, 1030-1057.
- Kellett, D.A., and Joyce, N., 2014. Analytical details of single- and multicollection  $^{40}\text{Ar}/^{39}\text{Ar}$  measurements for conventional step-heating and total-fusion age calculation using the Nu Noblesse at the Geological Survey of Canada. Geological Survey of Canada, Technical Note 8, 27 p.

- Kellett, D.A., Ryan, J.J., Colpron, M., Zagorevski, A., Joyce, N., and Zwingmann, H., 2017. Report of activities, 2017, for Yukon tectonic evolution – late Mesozoic to Tertiary: GEM2 Cordillera Project; Geological Survey of Canada, Open File 8306, 14 p. <https://doi.org/10.4095/305956>
- Kellett, D.A., Mottram, C., Banjan, M., Coutand, I., and Friend, M., 2018. Yukon tectonic evolution – late Mesozoic to Tertiary: GEM-2 Cordillera Project, report of activities 2018. Geological Survey of Canada, Open File 8470, 14 p., <https://doi.org/10.4095/311263>.
- Lee, J.-Y., Marti, K., Severinghaus, J.P., Kawamura, K., Yoo, H.-S., Lee, J.B., Kim, J.S., 2006. A redetermination of the isotopic abundances of atmospheric Ar. *Geochimica et Cosmochimica Acta* 70, 4507–4512.
- Long, D.G.F., 2015. Provenance and depositional framework of braided and meandering gravel-bed river deposits and associated coal deposits in active intermontane piggyback basins: The Upper Jurassic to Lower Cretaceous Tantalus Formation, Yukon. Yukon Geological Survey, Open File Report 2015-23, 80 p plus appendices.
- Ludwig, K.R., 2003. User's manual for Isoplot/Ex rev. 3.00: a Geochronological Toolkit for Microsoft Excel. Special Publication, 4, Berkeley Geochronology Center, Berkeley, 70 p.
- Min, K., Mundil, R., Renne, P.R. and Ludwig, K.R., 2000. A test for systematic errors in  $^{40}\text{Ar}/^{39}\text{Ar}$  geochronology through comparison with U/Pb analysis of a 1.1-Ga rhyolite. *Geochimica et Cosmochimica Acta*, 64(1), 73-98.
- Nelson, J.L., Colpron, M. and Israel, S., 2013. The Cordillera of British Columbia, Yukon, and Alaska: Tectonics and metallogeny. *Tectonics, Metallogeny, and Discovery: The North American Cordillera and Similar Accretionary Settings: Society of Economic Geologists Special Publication*, 17, 53-109.
- Renne, P.R., Mundil, R., Balco, G., Min, K. and Ludwig, K.R., 2010. Joint determination of  $^{40}\text{K}$  decay constants and  $^{40}\text{Ar}^*/^{40}\text{K}$  for the Fish Canyon sanidine standard, and improved accuracy for  $^{40}\text{Ar}/^{39}\text{Ar}$  geochronology. *Geochimica et Cosmochimica Acta*, 74(18), 5349-5367.
- Shirmohammad, F., Smith, P.L., Anderson, R.G., and McNicoll, V.J., 2011. The Jurassic succession at Lisadele Lake (Tulsequah map area, British Columbia, Canada) and its bearing on the tectonic evolution of the Stikine terrane. *Volumina Jurassica*, 2011, IX, 43-60.
- Stern, R.A., 1997. The GSC Sensitive High Resolution Ion Microprobe (SHRIMP): analytical techniques of zircon U-Th-Pb age determinations and performance evaluation: in *Radiogenic Age and Isotopic Studies*, Report 10, Geological Survey of Canada, Current Research 1997-F, 1-31.
- Stern, R.A., and Amelin, Y., 2003. Assessment of errors in SIMS zircon U-Pb geochronology using a natural zircon standard and NIST SRM 610 glass. *Chemical Geology*, 197, 111-146.
- Vermeesch, P., 2012. On the visualisation of detrital age distributions. *Chemical Geology*, 312, 190-194.

Vermeesch, P., 2018. IsoplotR: a free and open toolbox for geochronology. *Geoscience Frontiers*, 9(5), 1479-1493.